

Semilocal exchange-correlation potentials for solid-state calculations: Current status and future directions

Fabien Tran,¹ Jan Doumont,¹ Leila Kalantari,¹ Ahmad W. Huran,² Miguel A. L. Marques,² and Peter Blaha¹

¹*Institute of Materials Chemistry, Vienna University of Technology, Getreidemarkt 9/165-TC, A-1060 Vienna, Austria*

²*Institut für Physik, Martin-Luther-Universität Halle-Wittenberg, D-06099 Halle, Germany*

(Dated: 20 November 2021)

Kohn-Sham (KS) density functional theory (DFT) is a very efficient method for calculating various properties of solids as, for instance, the total energy, the electron density, or the electronic band structure. The KS-DFT method leads to rather fast calculations, however the accuracy depends crucially on the chosen approximation for the exchange and correlation (xc) functional E_{xc} and/or potential v_{xc} . Here, an overview of xc methods to calculate the electronic band structure is given, with the focus on the so-called semilocal methods that are the fastest in KS-DFT and allow to treat systems containing up to thousands of atoms. Among them, there is the modified Becke-Johnson potential that is widely used to calculate the fundamental band gap of semiconductors and insulators. The accuracy for other properties like the magnetic moment or the electron density, that are also determined directly by v_{xc} , is also discussed.

I. INTRODUCTION

The calculation of the properties of solids can be done very efficiently with the Kohn-Sham¹ (KS) method of density functional theory² (DFT). KS-DFT is clearly much faster than other methods, like for instance GW ,^{3,4} that are commonly used for calculating the quasiparticle band structure, or the random-phase approximation (RPA) and beyond^{5,6} for the total energy. Therefore, KS-DFT calculations on solids with a unit cell containing up to several thousands of atoms can be afforded. However, in KS-DFT a component in the total energy expression and in the effective potential in the corresponding KS equations, the one accounting for the exchange (x) and correlation (c) effects, has to be approximated. Exchange is due to the Pauli exclusion principle, while correlation arises due to a lowering of the energy by considering wavefunctions that are beyond the single determinant approximation in the Hartree-Fock theory. Since the reliability of the results obtained with KS-DFT depends mainly on the chosen xc functional, the search for more accurate approximate functionals is a very active field of research^{7–9} and several hundreds have been proposed so far.^{9,10} Most xc-functionals can be classified on the Jacob's ladder of John Perdew,^{11,12} where the first rung represents the most simple type of approximations and the highest rung the most sophisticated functionals. The rather general rule is that the functionals should, in principle, be more accurate, but also (this is the downside) computationally more expensive to evaluate when climbing up Jacob's ladder.

The properties of solids which are calculated directly from total energy are for instance the equilibrium geometry, the cohesive energy, or the formation enthalpy. For such calculations, a couple of xc functionals^{13–18} were or are considered as standard. Other properties depend more directly on the accuracy of the xc potential in the KS equations, such as the electronic band structure, the electron density, and magnetism, for which it may sometimes be necessary to use other types of xc approximations^{15,19–21} to get reliable results.

Here, the focus will be on the calculation of the electronic band structure of semiconductors and insulators with xc meth-

ods that are computationally the fastest, namely the so-called semilocal methods. Needless to say that quantities derived from the electronic band structure such as the band gap or the optical constants can serve as a guide for the design of more efficient materials for technological applications like photovoltaics,^{22,23} light emitting diodes,^{24,25} dynamic random access memory,²⁶ or thermoelectricity.²⁷ Among the semilocal methods, the modified Becke-Johnson potential proposed by two of us²⁰ has been shown to be very accurate for the calculation of the fundamental band gap. Comparison studies for the band gap (see Refs. 28–33 for the most exhaustive comparisons) have shown that the modified Becke-Johnson potential is on average more accurate than basically all other DFT methods, including the traditional hybrid functionals using a fixed fraction of Hartree-Fock exchange. Presently, only dielectric-function-dependent hybrid functionals^{34–37} and GW methods, in particular if applied self-consistently including vertex corrections,^{38,39} can lead to higher accuracy. However, since the modified Becke-Johnson potential is a DFT method, and furthermore was constructed empirically, the results are of course not systematically accurate. In addition, making a xc method accurate for a specific property (e.g., band gap), may deteriorate the description of other properties compared to more traditional methods.

The remainder of this paper is organized as follows. In Sec. II, a brief introduction to the KS-DFT method is given and the existing approximations for the xc potential v_{xc} are reviewed. Then, Sec. III provides a summary of the performance of various potentials for the electronic structure with a particular emphasis on the fundamental band gap. Results for other properties, e.g., the bandwidth, the magnetic moment, or the electron density, will also be mentioned. Finally, a summary is given in Sec. IV and ideas for further improvements are given in Sec. V.

II. THEORETICAL BACKGROUND

A. (Generalized) Kohn-Sham equations

In the KS-DFT method,¹ the total energy per unit cell of a periodic solid is given by

$$E_{\text{tot}} = T_s + \frac{1}{2} \int_{\text{cell}} v_{\text{Coul}}(\mathbf{r}) \rho(\mathbf{r}) d^3 r - \frac{1}{2} \sum_{\alpha}^{\text{cell}} Z_{\alpha} v_{\text{M}}^{\alpha}(\mathbf{R}_{\alpha}) + E_{\text{xc}}, \quad (1)$$

where

$$T_s = -\frac{1}{2} \sum_{\sigma} \sum_{n, \mathbf{k}} w_{n\mathbf{k}\sigma} \int_{\text{cell}} \psi_{n\mathbf{k}\sigma}^*(\mathbf{r}) \nabla^2 \psi_{n\mathbf{k}\sigma}(\mathbf{r}) d^3 r \quad (2)$$

is the noninteracting kinetic energy, the second and third terms represent the electrostatic interactions (electron-electron, electron-nucleus, and nucleus-nucleus) with

$$v_{\text{Coul}}(\mathbf{r}) = \int_{\text{crystal}} \frac{\rho(\mathbf{r}')}{|\mathbf{r} - \mathbf{r}'|} d^3 r' - \sum_{\beta}^{\text{crystal}} \frac{Z_{\beta}}{|\mathbf{r} - \mathbf{R}_{\beta}|} \quad (3)$$

and

$$v_{\text{M}}^{\alpha}(\mathbf{R}_{\alpha}) = \int_{\text{crystal}} \frac{\rho(\mathbf{r}')}{|\mathbf{R}_{\alpha} - \mathbf{r}'|} d^3 r' - \sum_{\beta \neq \alpha}^{\text{crystal}} \frac{Z_{\beta}}{|\mathbf{R}_{\alpha} - \mathbf{R}_{\beta}|} \quad (4)$$

being the Coulomb and Madelung potentials, respectively, and E_{xc} is the exchange-correlation energy. In Eqs. (1), (3), and (4), $\rho = \rho_{\uparrow} + \rho_{\downarrow}$ is the electron density, while Z_{α} and \mathbf{R}_{α} are the charge and position of the nuclei. In Eq. (2), n , \mathbf{k} , and σ are the band index, \mathbf{k} -point, and spin index, respectively, and $w_{n\mathbf{k}\sigma}$ is the product of the \mathbf{k} -point weight and the occupation number.

Searching for the Slater determinant which minimizes Eq. (1) yields the one-electron Schrödinger equations

$$\left(-\frac{1}{2} \nabla^2 + v_{\text{Coul}}(\mathbf{r}) + \hat{v}_{\text{xc},\sigma}(\mathbf{r}) \right) \psi_{n\mathbf{k}\sigma}(\mathbf{r}) = \epsilon_{n\mathbf{k}\sigma} \psi_{n\mathbf{k}\sigma}(\mathbf{r}) \quad (5)$$

that need to be solved self-consistently together with $\rho_{\sigma} = \sum_{n, \mathbf{k}} w_{n\mathbf{k}\sigma} |\psi_{n\mathbf{k}\sigma}|^2$. Within the strict KS framework, $\hat{v}_{\text{xc},\sigma}$ is calculated as the functional derivative of E_{xc} with respect to the electron density ρ_{σ} ($\hat{v}_{\text{xc},\sigma} = \delta E_{\text{xc}} / \delta \rho_{\sigma}$), which means that $\hat{v}_{\text{xc},\sigma}$ is a multiplicative potential ($\hat{v}_{\text{xc}} \psi_{n\mathbf{k}\sigma} = v_{\text{xc}} \psi_{n\mathbf{k}\sigma}$), i.e., it is the same for all orbitals. Instead, in the generalized KS (gKS) framework,⁴⁰ the derivative of E_{xc} is taken with respect to $\psi_{n\mathbf{k}\sigma}^*$ ($\hat{v}_{\text{xc}} \psi_{n\mathbf{k}\sigma} = \delta E_{\text{xc}} / \delta \psi_{n\mathbf{k}\sigma}^*$), which leads to a non-multiplicative xc operator (i.e., a potential that is different for each orbital $\psi_{n\mathbf{k}\sigma}$) in the case of functionals E_{xc} that do not depend only explicitly on ρ_{σ} .

Functionals whose ρ_{σ} -dependency is fully explicit are, for instance, the local density approximation (LDA)¹ and generalized gradient approximations (GGA). The most known examples of functionals that depend implicitly on ρ_{σ} are Hartree-Fock (HF) and the meta-GGAs (MGGA).⁴¹

As mentioned above, there are two types of xc potentials: multiplicative and non-multiplicative. In addition, among the multiplicative potentials $v_{\text{xc},\sigma}$ there are two distinctive subgroups, namely, those which are functional derivatives $v_{\text{xc},\sigma} = \delta E_{\text{xc}} / \delta \rho_{\sigma}$ of an energy functional E_{xc} and those which are not, but were modelled directly. Among the non-multiplicative potentials, the only ones we are aware of that are not obtained as functional derivative $\hat{v}_{\text{xc}} \psi_{n\mathbf{k}\sigma} = \delta E_{\text{xc}} / \delta \psi_{n\mathbf{k}\sigma}^*$ are the hybrids with a fraction of HF exchange that depends on a property of the system like the dielectric function (see, e.g. Refs. 34–36). The two next sections list some of the potentials which are the most relevant for the present work, i.e., for band gaps in particular. Then, in the third section a summary of what is known about the xc derivative discontinuity, which is strongly related to the band gap, is provided. Actually, we mention that we are here concerned with calculated band gaps that are obtained with the orbital energies, see Sec. II D for more discussion.

B. Multiplicative potentials

1. Potentials that are functional derivatives

We start by defining the xc-energy density per volume ϵ_{xc} ,

$$E_{\text{xc}} = \int_{\text{cell}} \epsilon_{\text{xc}}(\mathbf{r}) d^3 r, \quad (6)$$

which in LDA is a function of ρ_{σ} :

$$\epsilon_{\text{xc}}^{\text{LDA}}(\mathbf{r}) = \epsilon_{\text{xc}}^{\text{LDA}}(\rho_{\uparrow}(\mathbf{r}), \rho_{\downarrow}(\mathbf{r})), \quad (7)$$

while in GGA^{14,42} the first derivative of ρ_{σ} is also used:

$$\epsilon_{\text{xc}}^{\text{GGA}}(\mathbf{r}) = \epsilon_{\text{xc}}^{\text{GGA}}(\rho_{\uparrow}(\mathbf{r}), \rho_{\downarrow}(\mathbf{r}), \nabla \rho_{\uparrow}(\mathbf{r}), \nabla \rho_{\downarrow}(\mathbf{r})). \quad (8)$$

The functional derivative of LDA and GGA functionals is straightforwardly calculated with⁴³

$$v_{\text{xc},\sigma}^{\text{LDA}} = \frac{\delta E_{\text{xc}}^{\text{LDA}}}{\delta \rho_{\sigma}} = \frac{\partial \epsilon_{\text{xc}}^{\text{LDA}}}{\partial \rho_{\sigma}} \quad (9)$$

and

$$v_{\text{xc},\sigma}^{\text{GGA}} = \frac{\delta E_{\text{xc}}^{\text{GGA}}}{\delta \rho_{\sigma}} = \frac{\partial \epsilon_{\text{xc}}^{\text{GGA}}}{\partial \rho_{\sigma}} - \nabla \cdot \left(\frac{\partial \epsilon_{\text{xc}}^{\text{GGA}}}{\partial \nabla \rho_{\sigma}} \right), \quad (10)$$

respectively. From Eqs. (9) and (10), we can see that a GGA potential depends on ρ_{σ} and the first and second derivatives of ρ_{σ} , while $v_{\text{xc},\sigma}^{\text{LDA}}$ depends only on ρ_{σ} .

Among the functionals E_{xc} of the LDA type that will be considered for the discussion in Sec. III, there is the functional of the homogeneous electron gas^{1,44,45} (called LDA) and Sloc⁴⁶ (local Slater potential), which is an enhanced exchange LDA with no correlation and was proposed specifically for band gap calculations.

With something like 200 functionals, the GGAs represent the largest group of functionals,¹⁰ however only a couple of

them were shown to be interesting for the band gap. Among them, the three following are here considered. EV93PW91, which consists of the exchange EV93 of Engel and Vosko⁴⁷ that we combined with PW91 correlation¹³ in our previous works.^{29,48} The EV93 exchange was constructed to reproduce the exact exchange (EXX) potential in atoms. AK13 from Armiento and Kümmel,⁴⁹ a parameter-free exchange functional that was constructed to have a potential that changes discontinuously at integer particle numbers. In our previous works,²⁹ as well as in others,⁵⁰ AK13 was used with no correlation added. In the recently proposed GGA HLE16,⁵¹ the parameters were tuned in order to give accurate band gaps. Of course, the standard GGA for solids of Perdew *et al.*¹⁴ (PBE), which is known to be very inaccurate for band gaps,⁵² will also be considered [note that a simple relationship between PBE and one-shot *GW* (G_0W_0) band gaps was proposed in Ref. 53]. Other standard GGAs like BLYP^{42,54} or PBEsol¹⁷ lead to results for the electronic structure that are very similar to PBE⁵⁵ and, therefore, do not need to be considered.

The other families of pure DFT approximations for E_{xc} like the $\nabla^2\rho$ -MGGa functionals⁴¹ which depend on the second derivative of ρ , the nonlocal van der Waals functionals,⁵⁶ or the weighted-density approximation^{57,58} are not considered in the present work. We just mention that the latter two approximations are more complicated since ε_{xc} is itself an integral:

$$\varepsilon_{xc}(\mathbf{r}) = \int_{\text{crystal}} f(\rho(\mathbf{r}), \rho(\mathbf{r}'), \nabla\rho(\mathbf{r}), \nabla\rho(\mathbf{r}'), |\mathbf{r} - \mathbf{r}'|) d^3r', \quad (11)$$

which brings full nonlocality (they are beyond the semilocal approximations), but also leads to more complicated implementations and expensive calculations.

2. Potentials that are not functional derivatives

A couple of potentials v_{xc} were directly modelled in order to produce accurate results for a given property, typically related to the electronic structure, like the band gap. Such potentials having no associated energy functional E_{xc} were named *stray* by Gaiduk *et al.*⁵⁹

Presenting such potentials chronologically, we start with LB94,⁶⁰ which reads

$$v_{xc,\sigma}^{\text{LB94}}(\mathbf{r}) = v_{xc,\sigma}^{\text{LDA}}(\mathbf{r}) - \beta \rho_{\sigma}^{1/3}(\mathbf{r}) \frac{y_{\sigma}^2(\mathbf{r})}{1 + 3\beta y_{\sigma}(\mathbf{r}) \text{arcsinh}(y_{\sigma}(\mathbf{r}))}, \quad (12)$$

where $y_{\sigma} = |\nabla\rho_{\sigma}|/\rho_{\sigma}^{4/3}$ and $\beta = 0.05$. LB94 was constructed such that the asymptotic behavior at $|\mathbf{r}| \rightarrow \infty$ in finite systems is $-1/|\mathbf{r}|$ as it should be. Note that in Ref. 61, a slight modification of LB94 (LB94 α) was proposed, where $\beta = 0.01$ and the exchange $v_{xc,\sigma}^{\text{LDA}}$ is multiplied by $\alpha = 1.19$. From Eq. (12), we can see that the LB94 potential depends on the first derivative of ρ_{σ} , but not on the second derivative like the GGA potentials do.

Becke and Johnson⁶² (BJ) proposed an approximation to

the EXX potential in atoms that is given by

$$v_{x,\sigma}^{\text{BJ}}(\mathbf{r}) = v_{x,\sigma}^{\text{BR}}(\mathbf{r}) + \frac{1}{\pi} \sqrt{\frac{5}{6}} \sqrt{\frac{t_{\sigma}(\mathbf{r})}{\rho_{\sigma}(\mathbf{r})}}, \quad (13)$$

where

$$v_{x,\sigma}^{\text{BR}}(\mathbf{r}) = -\frac{1}{b_{\sigma}(\mathbf{r})} \left(1 - e^{-x_{\sigma}(\mathbf{r})} - \frac{1}{2} x_{\sigma}(\mathbf{r}) e^{-x_{\sigma}(\mathbf{r})} \right) \quad (14)$$

is the Becke-Roussel (BR) potential⁶³ with x_{σ} that is obtained by solving a nonlinear equation involving ρ_{σ} , $\nabla\rho_{\sigma}$, $\nabla^2\rho_{\sigma}$, and the kinetic-energy density $t_{\sigma} = (1/2) \sum_{n,\mathbf{k}} w_{n\mathbf{k}\sigma} \nabla\psi_{n\mathbf{k}\sigma}^* \cdot \nabla\psi_{n\mathbf{k}\sigma}$. Then, in Eq. (14) $b_{\sigma} = [x_{\sigma}^3 e^{-x_{\sigma}} / (8\pi\rho_{\sigma})]^{1/3}$. Note that in Refs. 62–64 the BR potential was shown to reproduce very accurately the Slater potential,⁶⁵ which is the hole component of the EXX potential. Since the BJ potential depends on t_{σ} it can be considered as a MGGa, although it is somehow abusive since the mathematical structure of $v_{x,\sigma}^{\text{BJ}}$ differs significantly from the true MGGa potentials discussed in Sec. II C. The BJ potential has attracted a lot of interest and has been studied^{48,66–68} or modified^{20,55,69–72} by a certain number of groups.

In particular, among these variants of the BJ potential there is the aforementioned mBJLDA xc potential that was introduced in Ref. 20 as an alternative to the expensive *GW* and hybrid methods for calculating band gaps. mBJLDA consists of a modification of the BJ potential (mBJ) for exchange and LDA^{44,45} for the correlation potential. The mBJ exchange is given by

$$v_{x,\sigma}^{\text{mBJ}}(\mathbf{r}) = c v_{x,\sigma}^{\text{BR}}(\mathbf{r}) + (3c - 2) \frac{1}{\pi} \sqrt{\frac{5}{6}} \sqrt{\frac{t_{\sigma}(\mathbf{r})}{\rho_{\sigma}(\mathbf{r})}}, \quad (15)$$

where c is a functional of the density and is given by

$$c = \alpha + \beta \sqrt{g}, \quad (16)$$

where

$$g = \frac{1}{V_{\text{cell}}} \int_{\text{cell}} \frac{1}{2} \left(\frac{|\nabla\rho^{\uparrow}(\mathbf{r}')|}{\rho^{\uparrow}(\mathbf{r}')} + \frac{|\nabla\rho^{\downarrow}(\mathbf{r}')|}{\rho^{\downarrow}(\mathbf{r}')} \right) d^3r' \quad (17)$$

is the average of $|\nabla\rho_{\sigma}|/\rho_{\sigma}$ in the unit cell. It is important to underline that using g brings some kind of nonlocality since the value of $v_{x,\sigma}^{\text{mBJ}}$ at \mathbf{r} depends on $|\nabla\rho_{\sigma}|/\rho_{\sigma}$ at every point in space (thus, mBJLDA is not strictly speaking a semilocal method). However, this nonlocality is different from the true nonlocality as in Eq. (11) or in the HF method (see Sec. II C 1), where there is a dependency on the interelectronic distance $|\mathbf{r} - \mathbf{r}'|$. The values of α and β in Eq. (16) were determined to be $\alpha = -0.012$ (dimensionless) and $\beta = 1.023 \text{ bohr}^{1/2}$ by minimizing the mean absolute error of the band gap for a group of solids.²⁰ Subsequently, other parametrizations for α and β have been proposed in Ref. 73 for semiconductors with band gaps smaller than 7 eV or in Refs. 74 and 75 for halide perovskites. Note that in the literature, the mBJLDA potential

is sometimes called TB-mBJ,⁷⁶ TB,⁷⁷ or TB09,^{10,34,78} which refers to the authors of the method.

A very interesting potential for band gap calculations was proposed by Kuisma *et al.*²¹ Their potential, which is based on the potential proposed by Gritsenko *et al.*⁷⁹ (GLLB), is given by (SC stands for solid and correlation)

$$v_{xc,\sigma}^{\text{GLLB-SC}}(\mathbf{r}) = 2e_{x,\sigma}^{\text{PBEsol}}(\mathbf{r}) + K_x^{\text{LDA}} \times \sum_{n,\mathbf{k}} w_{n\mathbf{k}\sigma} \sqrt{\epsilon_{\text{H}} - \epsilon_{n\mathbf{k}\sigma}} \frac{|\psi_{n\mathbf{k}\sigma}(\mathbf{r})|^2}{\rho_{\sigma}(\mathbf{r})} + v_{c,\sigma}^{\text{PBEsol}}(\mathbf{r}), \quad (18)$$

where $e_{x,\sigma}^{\text{PBEsol}}$ is the PBEsol exchange-energy density per spin- σ electron [defined by $E_x = \sum_{\sigma} \int_{\text{cell}} e_{x,\sigma}(\mathbf{r}) \rho_{\sigma}(\mathbf{r}) d^3r$], $v_{c,\sigma}^{\text{PBEsol}} = \delta E_c^{\text{PBEsol}} / \delta \rho_{\sigma}$ is the PBEsol correlation potential, and $K_x^{\text{LDA}} = 8\sqrt{2}/(3\pi^2)$. The particularity of the GLLB-SC potential is to depend on the orbital energies [ϵ_{H} is for the highest occupied one, i.e., at the valence band maximum (VBM)]. It is easy to show⁸⁰ that the dependency on ϵ_{H} in Eq. (18) leads to the possibility to calculate the exchange part of the derivative discontinuity, that is given by

$$\Delta_x^{\text{GLLB-SC}} = \int_{\text{cell}} \psi_L^*(\mathbf{r}) \left[\sum_{n,\mathbf{k}} K_x^{\text{LDA}} w_{n\mathbf{k}\sigma_L} (\sqrt{\epsilon_L - \epsilon_{n\mathbf{k}\sigma_L}} - \sqrt{\epsilon_{\text{H}} - \epsilon_{n\mathbf{k}\sigma_L}}) \frac{|\psi_{n\mathbf{k}\sigma_L}(\mathbf{r})|^2}{\rho_{\sigma_L}(\mathbf{r})} \right] \psi_L(\mathbf{r}) d^3r, \quad (19)$$

where ψ_L is the lowest unoccupied orbital [conduction band minimum (CBM)] and σ_L its spin value.

Among the other computationally fast model potentials proposed in the literature that are not considered in the present work, we mention the exchange potentials of Lembarki *et al.*⁸¹ and Harbola and Sen,⁸² which, as LB94, depend on ρ_{σ} and $\nabla \rho_{\sigma}$. The exchange potential of Umezawa⁸³ depends on ρ_{σ} and $\nabla \rho_{\sigma}$, but also on the Fermi-Amaldi potential⁸⁴ which depends on the number of electrons N such that its application to solids is unclear. In Ref. 85, Ferreira *et al.* proposed the LDA-1/2 method, which improves upon LDA for band gaps. However, the method is not always straightforward to apply and ambiguities may arise depending on the case (see Refs. 86 and 87). A few other model potentials can be found in the work of Staroverov.⁶⁷

We also mention that stray potentials have undesirable features both at the fundamental and practical level as shown in Refs. 59, 68, and 88.

Last but not least, we mention that some of the potentials presented in this section (LB94, BJ, and mBJ) and in the previous one (e.g., AK13) were shown to lead to numerical problems in the asymptotic region far from nuclei in finite systems.^{89,90}

C. Non-multiplicative potentials

1. Potentials that are functional derivatives

We begin with the MGGA functionals that use the kinetic-energy density t_{σ} as additional ingredient compared to the GGAs (here, we do not consider MGGA's which depend on $\nabla^2 \rho$):

$$\epsilon_{xc}^{\text{MGGA}} = \epsilon_{xc}^{\text{MGGA}}(\rho_{\uparrow}, \rho_{\downarrow}, \nabla \rho_{\uparrow}, \nabla \rho_{\downarrow}, t_{\uparrow}, t_{\downarrow}). \quad (20)$$

Since there is, via t_{σ} , an implicit dependency on ρ_{σ} , the functional derivative of E_{xc}^{MGGA} with respect to ρ_{σ} can not be calculated (at least not in a straightforward way). Instead, the functional derivative with respect to $\psi_{n\mathbf{k}\sigma}^*$ is taken,^{91,92} which gives

$$\begin{aligned} \hat{v}_{xc,\sigma}^{\text{MGGA}} \psi_{n\mathbf{k}\sigma} &= \frac{\partial \epsilon_{xc}^{\text{MGGA}}}{\partial \rho_{\sigma}} \psi_{n\mathbf{k}\sigma} - \left(\nabla \cdot \frac{\partial \epsilon_{xc}^{\text{MGGA}}}{\partial \nabla \rho_{\sigma}} \right) \psi_{n\mathbf{k}\sigma} \\ &\quad - \frac{1}{2} \nabla \cdot \left(\frac{\partial \epsilon_{xc}^{\text{MGGA}}}{\partial t_{\sigma}} \nabla \psi_{n\mathbf{k}\sigma} \right) \\ &= v_{xc,\sigma}^{\text{GGA-part}} \psi_{n\mathbf{k}\sigma} - \frac{1}{2} \nabla \cdot \left(\frac{\partial \epsilon_{xc}^{\text{MGGA}}}{\partial t_{\sigma}} \nabla \psi_{n\mathbf{k}\sigma} \right), \end{aligned} \quad (21)$$

where the last term, which is non-multiplicative, arises due to the dependency on t_{σ} . Among the numerous MGGA functionals that have been proposed,⁴¹ some of them have been shown to improve clearly over the standard PBE for the geometry and energetics of electronic systems. This includes SCAN¹⁸ and MVS⁹³ (tested in Refs. 94 and 95 for the band gap), as well as HLE17⁹⁶ and revM06-L.⁹⁷

Another class of functionals that lead to a non-multiplicative potential, but not of the semilocal type, is HF and the (screened) hybrid functionals, where a fraction α_x of semilocal exchange is replaced by HF exchange:

$$\epsilon_{xc}^{\text{hybrid}}(\mathbf{r}) = \epsilon_{xc}^{\text{SL}}(\mathbf{r}) + \alpha_x [\epsilon_x^{(\text{scr})\text{HF}}(\mathbf{r}) - \epsilon_x^{(\text{scr})\text{SL}}(\mathbf{r})], \quad (22)$$

where

$$\begin{aligned} \epsilon_x^{(\text{scr})\text{HF}}(\mathbf{r}) &= -\frac{1}{2} \sum_{\sigma} \sum_{n,\mathbf{k}} \sum_{n',\mathbf{k}'} w_{n\mathbf{k}\sigma} w_{n'\mathbf{k}'\sigma} \psi_{n\mathbf{k}\sigma}^*(\mathbf{r}) \psi_{n'\mathbf{k}'\sigma}(\mathbf{r}) \\ &\quad \times \int_{\text{crystal}} v(|\mathbf{r} - \mathbf{r}'|) \psi_{n'\mathbf{k}'\sigma}^*(\mathbf{r}') \psi_{n\mathbf{k}\sigma}(\mathbf{r}') d^3r', \end{aligned} \quad (23)$$

which is a fully nonlocal exchange-energy density. The functional derivative of $E_x^{(\text{scr})\text{HF}}$ with respect to $\psi_{n\mathbf{k}\sigma}^*$ is given by

$$\begin{aligned} \hat{v}_{x,\sigma}^{(\text{scr})\text{HF}} \psi_{n\mathbf{k}\sigma}(\mathbf{r}) &= - \sum_{n',\mathbf{k}'} w_{n'\mathbf{k}'\sigma} \psi_{n'\mathbf{k}'\sigma}(\mathbf{r}) \\ &\quad \times \int_{\text{crystal}} v(|\mathbf{r} - \mathbf{r}'|) \psi_{n'\mathbf{k}'\sigma}^*(\mathbf{r}') \psi_{n\mathbf{k}\sigma}(\mathbf{r}') d^3r'. \end{aligned} \quad (24)$$

In Eqs. (23) and (24), v can be either the bare Coulomb potential $v = 1/|\mathbf{r} - \mathbf{r}'|$ or a potential that is screened at short

or long range. In the case of solids, it is computationally advantageous to use a potential that is short range, i.e., the long-range part is screened. Such short-range potentials are the Yukawa potential $v = e^{-\lambda|\mathbf{r}-\mathbf{r}'|}/|\mathbf{r}-\mathbf{r}'|$ (Ref. 98) or $v = \text{erfc}(\mu|\mathbf{r}-\mathbf{r}'|)/|\mathbf{r}-\mathbf{r}'|$ where erfc is the complementary error function (Ref. 15). Due to the nonlocal character of Eqs. (23) and (24) as well as the summations over the occupied orbitals, the HF/hybrid methods lead to calculations that are one or several orders of magnitude more expensive than with semilocal approximations. However, similarly as G_0W_0 , hybrids can be applied non-self-consistently, which can be a very good approximation for the band gap.^{99,100} The most popular hybrid functional in solid-state physics is HSE06 from Heyd *et al.*,^{15,101} which uses the Coulomb operator screened with the erfc function and the PBE functional for the semilocal part in Eq. (22). Another well-known hybrid functional is B3PW91,¹⁰² which has been shown to perform very well for band gaps similarly as HSE06.^{29,103}

Another type of non-multiplicative potentials that are not considered here are those of the self-interaction corrected functionals.¹⁰⁴ We also note that the DFT+ U ¹⁹ and on-site-hybrid^{105,106} methods also lead to non-multiplicative potentials, however they are somehow crude approximations to the HF/hybrid methods.

We mention that in principle the functional derivative with respect to ρ can also be calculated for implicit functionals of ρ . However, the equations of the optimized effective potential^{7,107–109} (OEP) need to be solved, which, depending on the type of basis set, can be quite cumbersome (see, e.g., Ref. 110) in particular since the response function, that involves the unoccupied orbitals, is required.

To finish, we also mention that MGGA functionals can be *deorbitalized* by replacing t_σ in Eq. (20) by an approximate expression that depends on ρ_σ and its two first derivatives.^{111–114} This leads to $\nabla^2\rho$ -MGGA that are pure DFT functionals with a potential v_{xc} that can be readily calculated, but that involves up to the fourth derivative of ρ_σ .

2. Potentials that are not functional derivatives

Non-multiplicative potentials that are not obtained as a functional derivative, but were directly modelled are the hybrids with a fraction α_x of HF exchange that depends on a property of the system like the dielectric function^{34–37,115–118} or the electron density like in Eq. (17).^{34,35} To our knowledge, no non-multiplicative potential of the semilocal type has been proposed.

D. Derivative discontinuity

In KS-DFT,

$$E_g^{\text{KS}} = \varepsilon_L - \varepsilon_H \quad (25)$$

is called the KS band gap, which, in *exact* KS-DFT, is not equal to the fundamental band gap defined as (N is the number

of electrons in the system)

$$\begin{aligned} E_g &= I(N) - A(N) \\ &= [E_{\text{tot}}(N-1) - E_{\text{tot}}(N)] - [E_{\text{tot}}(N) - E_{\text{tot}}(N+1)], \end{aligned} \quad (26)$$

where I and A are the ionization potential and electron affinity, respectively. The two gaps differ by the so-called xc derivative discontinuity Δ_{xc} .^{119,120}

$$\begin{aligned} E_g &= I(N) - A(N) = -\varepsilon_H(N) - [-\varepsilon_H(N+1)] \\ &= \underbrace{\varepsilon_L(N) - \varepsilon_H(N)}_{E_g^{\text{KS}}} + \underbrace{\varepsilon_H(N+1) - \varepsilon_L(N)}_{\Delta_{xc}} = E_g^{\text{KS}} + \Delta_{xc}, \end{aligned} \quad (27)$$

where we have used the fact that $I(N) = -\varepsilon_H(N)$ ¹²¹ in exact KS-DFT. Δ_{xc} is positive and numerical examples (see Refs. 122–124 for results on solids) strongly indicate that Δ_{xc} can be of the same order of magnitude as E_g^{KS} , i.e., the exact E_g^{KS} is much smaller than the experimental band gap $E_g = E_g^{\text{expt}}$.

Concerning approximate xc methods, a brief summary of some of the most important points from Refs. 7, 125–127 is the following:

- **LDA, GGA:** Like with exact KS-DFT, using the orbital energies [Eq. (25)] (i.e., ignoring Δ_{xc}) leads to band gaps that are much smaller than experiment with most LDA/GGA functionals for both finite systems and solids. For finite systems, using the total energies [Eq. (26)] or methods^{128–131} to calculate Δ_{xc} with the LDA/GGA quantities (and add it to E_g^{KS}) gives much better agreement with experiment. According to our knowledge, for solids there is no method providing a non-zero Δ_{xc} within a LDA/GGA framework. Actually, in Ref. 131 it is shown that $\Delta_{xc} = E_g - E_g^{\text{KS}} = 0$ in solids (see also Ref. 130), which also means that using Eq. (26) does not help. Specialized GGA functionals^{49,51} can lead to band gaps calculated with Eq. (25) that agree quite well with experiment.
- **Non-multiplicative potentials:** Potentials of the MGGA and HF/hybrid functionals implemented within the gKS method lead to a gKS gap $E_g^{\text{gKS}} = \varepsilon_L - \varepsilon_H$ that contains a portion of Δ_{xc} . For instance, with hybrid functionals [Eq. (22)], a fraction α_x of Δ_x is included in E_g^{gKS} . Thus, this is one of the reasons why E_g^{gKS} can be larger (and in better agreement with experiment) than E_g^{KS} calculated from standard LDA/GGA multiplicative potentials.
- **Multiplicative potentials obtained from the OEP method:** For a given non-pure-DFT functional (MGGA, HF/hybrid, or RPA), the multiplicative potential leads to a KS gap E_g^{KS} that is usually smaller than its counterpart E_g^{gKS} , since $E_g^{\text{gKS}} - E_g^{\text{KS}} \approx \Delta_{xc}$ that should be positive in principle. However, with MGGA functionals a negative Δ_{xc} can sometimes be obtained.^{94,132}

From above, an important point is that it is in principle not correct to compare E_g^{KS} with the experimental E_g^{expt} when the orbital energies were obtained with a multiplicative potential. With such potentials, a Δ_{xc} should be added to E_g^{KS} before comparing with E_g^{expt} (however with LDA/GGA for solids one may argue that it is not necessary since $\Delta_{xc} = 0$). Theoretically, it is also not very sound to devise multiplicative potentials that give E_g^{KS} in agreement with E_g^{expt} (mBJLDA and HLE16 are such examples), since it means that these potentials will most likely be very different from the exact multiplicative potential. Forcing an agreement between E_g^{KS} and E_g^{expt} may result in a potential with unphysical features leading to quite inaccurate results for properties other than the band gap, as shown in Refs. 32, 75, and 133.

Thus, among the fast semilocal methods, the GLLB-SC potential (Δ_{xc} can be calculated) and the non-multiplicative MGGa potentials (Δ_{xc} included in $\epsilon_L - \epsilon_H$) are from a formal point of view much more appealing than potentials like mBJLDA or HLE16.

III. OVERVIEW OF RESULTS

A. Fundamental band gap

The fundamental band gap is very often the quantity one is interested in when calculating the electronic band structure of a semiconducting or insulating solid, and $GW^{3,4}$ is often considered as the current state-of-the-art method. However, despite recent advances in the speedup of GW methods,^{134–136} the calculations are not yet routinely applied to large systems. Furthermore, with one-shot G_0W_0 , the results may depend on the used orbitals, which is particularly the case for antiferromagnetic (AFM) oxides.¹³⁷ Also, the convergence with respect to the number of unoccupied orbitals may be difficult to achieve.^{138–140} Alternatively, hybrid functionals can be used, but they are also very expensive, albeit less than the GW methods. As already mentioned above, there exist semilocal methods that are able to provide band gaps with an accuracy that can be comparable to GW or hybrids depending on the test set. A certain number of benchmark calculations for large test sets of solids were done, and below we summarize the results for some of them.

1. Test set of 76 solids

In two of our previous works,^{29,32} a set of 76 solids was build and used for benchmarking and comparing twelve different DFT methods in total. The tested methods are two LDA-type functionals (LDA and SloC), four GGAs (PBE, EV93PW91, AK13, and HLE16), two MGGAs (BJLDA and mBJLDA), LB94, GLLB-SC, and two hybrids (HSE06 and B3PW91). The test set (see Fig. 1) consists of a large variety of semiconductors and insulators, most of them being IVA solids, IIIA-VA compounds, transition-metal (TM) chalcogenides/halides, rare gases, or ionic IA-VIIA or IIA-

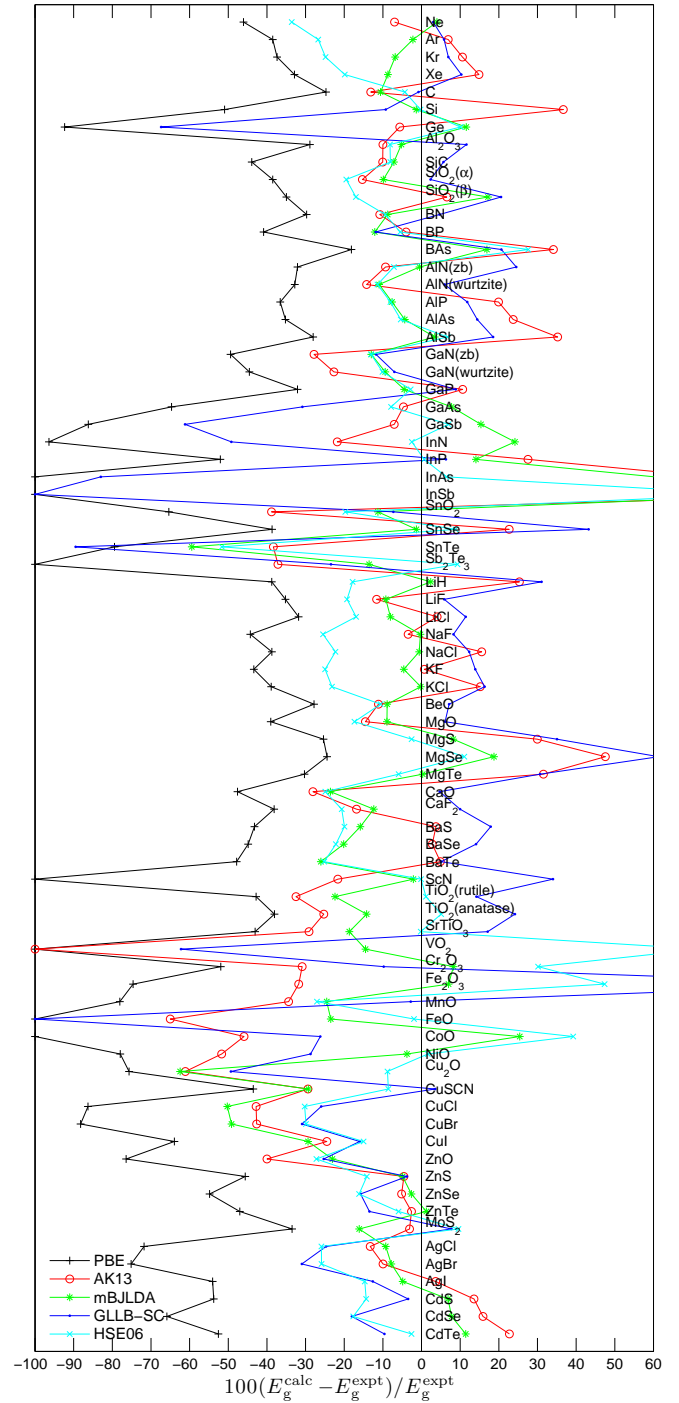


FIG. 1. Relative error (in %) with respect to experiment in the fundamental band gap for the set of 76 solids. The values can be found in Refs. 29 and 32.

VIA compounds. Among the TM oxides, six of them (Cr_2O_3 , Fe_2O_3 , MnO , FeO , CoO , and NiO) are AFM with strongly correlated $3d$ electrons. Also included in the set is VO_2 that has been extensively studied (see, e.g. Ref. 141). Here, the non-magnetic phase of VO_2 is considered. The calculations were done with the WIEN2K all-electron code,¹⁴² which is

TABLE I. Mean errors with respect to experiment for the band gap of 76 solids obtained with various DFT methods. The M(A)E is in eV and the M(A)RE is in %. The results, obtained with the WIEN2K code, are from Ref. 32 for BJDLa, LB94, and GLLB-SC, and Ref. 29 for all other methods.

	LDA	PBE	EV93PW91	AK13	Sloc	HLE16	BJLDA	mBJLDA	LB94	GLLB-SC	HSE06	B3PW91
ME	-2.17	-1.99	-1.55	-0.28	-0.76	-0.82	-1.53	-0.30	-1.87	0.20	-0.68	-0.36
MAE	2.17	1.99	1.55	0.75	0.90	0.90	1.53	0.47	1.88	0.64	0.82	0.73
MRE	-58	-53	-35	-6	-21	-20	-41	-5	-54	-4	-7	6
MARE	58	53	36	24	30	25	41	15	55	24	17	23

based on the linearized-augmented plane-wave basis set.¹⁴³ We mention that the HSE06 results were actually obtained with YS-PBE0,¹⁴⁴ which is also a screened hybrid functional and was shown to lead to basically the same results as HSE06 for the electronic structure.¹⁴⁴ As in Refs. 29 and 32, we have decided to use the acronym HSE06.

The mean errors with respect to experiment^{28,35,36,103,145–151} are reported in Table I, where M(R)E and MA(R)E denote the mean (relative) and mean absolute (relative) error, respectively. Here, we summarize only the most important observations from Refs. 29 and 32. With a MAE around 2 eV, the most inaccurate xc methods are LDA, PBE, and LB94. EV93PW91 and BJDLa are only slightly better with MAE \sim 1.5 eV. For the more accurate methods, the ranking depends on whether the MAE or the MARE is considered, however for both quantities mBJLDA is the most accurate method with MAE = 0.47 eV and MARE = 15%. The hybrid HSE06 has also a very low MARE (17%), while GLLB-SC is the second most accurate method in terms of MAE (0.64 eV).

The detailed results for the 76 solids are shown graphically on Figs. 1 and 2 for selected methods. As LDA, PBE systematically underestimates the band gap and this is particularly severe for small band gaps. mBJLDA does not show a pronounced trend towards underestimation or overestimation, such that the ME and MRE are among the smallest. However, mBJLDA does not perform well for the Cu¹⁺ compounds (e.g., Cu₂O) and ZnO, but these are basically the only systems for which mBJLDA clearly fails. While GLLB-SC works much better than mBJLDA for the Cu¹⁺ compounds, it strongly underestimates the band gaps in the heavy IIIA-VA semiconductors like InSb by nearly 100%, but also strongly overestimates in a few cases like MgSe and Fe₂O₃. The expensive hybrid HSE06 is very accurate for band gaps smaller than \sim 7 eV, but clearly underestimates larger band gaps [see Fig. 2(a)]. Note that mBJLDA, GLLB-SC, and HSE06 underestimate the band gap of ZnO by a similar amount (\sim 1 eV).

For the particular case of strongly correlated AFM solids, the mBJLDA results should be considered as excellent and clearly more accurate than all other semilocal methods. Only HSE06 is of similar accuracy. Concerning non-magnetic VO₂, we mention that in Refs. 141 and 152 it is shown that mBJLDA and HSE06 lead to a correct description of the electronic structure of the (insulating) rutile and (metallic) monoclinic phases, while LDA and PBE do not.

2. Test set of 472 solids

Very recently, a large-scale benchmark study for the band gap was done by some of us.³³ The data set consists of 472 solids and, as for the one discussed in the previous section, it consists of a large variety of solids. Nevertheless, this test set contains no strongly correlated AFM TM oxides. The calculations from Ref. 33 were done with the VASP code, which uses the projector augmented wave formalism.^{153,154} Additional calculations with the EV93PW91, AK13, and GLLB-SC (and again PBE) methods were performed for the present work using the WIEN2K code. The detailed WIEN2K results are in Table SI of the supplementary material. Here, we mention that the agreement between VASP and WIEN2K band gaps is in general excellent for standard functionals like LDA or PBE. However, for a couple of solids, those with very large band gaps like the rare gases, noticeably larger disagreement can be obtained with other xc methods like mBJLDA or HLE16. In such cases, the discrepancy can be of the order of the eV, which however, has no real impact on the conclusion.

A summary of the statistics for the error is shown in Table II, and the data for the band gaps smaller than 10 eV are shown in Fig. 3 for selected methods (see Figs. S1-S11 of the supplementary material for all methods and the full range of band gap values). The mBJLDA, AK13, HLE16, and HSE06 methods lead to the lowest MAE and MARE, which are \sim 0.5 eV and 30-35%, respectively. These four methods can be considered as performing equally well. For the test set discussed in Sec. III A 1, the mBJLDA potential was shown to be clearly more accurate, in particular in terms of MAE. Two reasons may explain why this is not the case for the large test set. First, the errors (in eV, but not in %) with HSE06 are clearly smaller for small band gaps, and since the test set of 472 solids contains (many) more such small band gaps (mainly around 2 eV), it favors HSE06. Regarding AK13 and HLE16, the second reason may be due to the fact that TM oxides, considered in Sec. III A 1, but not here, are very well described by mBJLDA, but not with AK13 and HLE16.

The other functionals are less accurate. We remark that BJDLa and SCAN lead to quasi-identical mean errors (MAE = 0.8 eV and MARE = 36-38%), and that the screened hybrid HSE06 is much more accurate than the unscreened PBE0. A much more detailed discussion of the results can be found in Ref. 33.

TABLE II. Mean errors with respect to experiment for the band gap of 472 solids obtained with various DFT methods. The M(A)E is in eV and the M(A)RE is in %. The results are from Ref. 33 and were obtained with the VASP code for all methods, except those for EV93PW91, AK13, and GLLB-SC that were obtained with the WIEN2K code for the present work.

	LDA	PBE	EV93PW91	AK13	HLE16	BJLDA	mBJLDA	SCAN	GLLB-SC	HSE06	PBE0
ME	-1.1	-1.0	-0.7	-0.1	-0.4	-0.7	-0.2	-0.7	0.4	-0.1	0.5
MAE	1.2	1.1	0.8	0.5	0.6	0.8	0.5	0.8	0.7	0.5	0.8
MRE	-47	-41	-22	9	-7	-27	-2	-27	16	10	53
MARE	51	46	36	35	32	36	30	38	39	31	61

3. Other benchmark studies

Among the xc methods tested for the band gap with the sets of 76 and 472 solids (discussed above), SCAN is the only one consisting of a MGGA energy functional with a potential implemented in the gKS framework. Such MGGA methods are extremely promising for band gap calculation since they are of the semilocal type (and therefore computationally fast) and lead to a non-zero xc derivative discontinuity, allowing for a theoretically justified comparison of the gKS band gap E_g^{gKS} with the experimental E_g .

As discussed above, SCAN is inferior to the semilocal methods that were designed specifically for band gaps (mBJLDA and HLE16) for the set of 472 solids. However, many other MGGA functionals have been proposed, and several of them have been tested for band gaps in Refs. 52, 94–97, 112, 145, 155–161. In most of these studies, the test sets are of smaller size (up to 40 solids) and contain no AFM solids, such that a direct comparison of the mean errors with our two previous benchmarks is not possible. However, it should be possible to get a rough idea of the performance of these MGGAs with respect to mBJLDA or GLLB-SC, which were not considered in these studies.

Truhlar and co-workers have proposed several MGGA functionals that have been tested on band gaps. Among them, an interesting one is HLE17,⁹⁶ which shows a performance that is similar to the GGA HLE16 and hybrid HSE06.⁹⁶ For the three functionals, the MAE is 0.30–0.32 eV for a set of 31 semiconductors. For this test set, mBJLDA leads to a MAE of 0.27 eV. However, for the AFM TM monoxides MnO, FeO, CoO, and NiO, HLE17 is clearly worse than HSE06 and mBJLDA by providing band gaps that are too small by 1–2 eV with respect to experiment. Nevertheless, HLE17 is better than SCAN according to the results in Ref. 162. In Ref. 97, the MGGA revM06-L was shown to perform better than a certain number of other functionals for the same set of 31 semiconductors. However, the MAE is 0.45 eV, which is larger than HLE17.

To date, HLE17 seems to be the most accurate MGGA (implemented within a gKS framework) according to our knowledge. However, HLE17 is slightly inferior to mBJLDA for the test set of 31 semiconductors and does not perform well for the AFM oxides. Other standard MGGA functionals like TPSS¹⁶³ or revTPSS,¹⁶⁴ or the recent one from Tao and Mo¹⁶⁵ barely improve over PBE (see, e.g., Ref. 95). Also noteworthy is a very recent MGGA functional proposed by Patra *et al.*¹⁶¹ leading to a MAE of 0.69 eV for a set of 67 solids (comprising

no AFM TM oxides), which is, however, larger than 0.44 eV obtained with mBJLDA for the same test set.

A short summary of other benchmark studies involving the mBJLDA potential is now given. Jiang¹⁶⁶ compared PBE and mBJLDA on a set of 50 solids, which includes TM dichalcogenides and Ti-containing oxides. As expected mBJLDA is much more accurate than PBE. Another goal of this work was to evaluate the accuracy of the non-self-consistent calculation of the mBJLDA band gap, which consists of one iteration on top of a PBE calculation (mBJLDA@PBE). In most cases, the difference between the mBJLDA and mBJLDA@PBE band gaps is below 0.1 eV. The difference is much larger in rare-gas solids, e.g., Ne where the band gap with mBJLDA@PBE is smaller than the self-consistent one by 4.5 eV. Another case is ZnO where this time the mBJLDA@PBE band gap is larger by ~ 0.5 eV. It is also found that mBJLDA@PBE is only slightly less accurate than one-shot G_0W_0 for the TM dichalcogenides.

Lee *et al.*²⁸ calculated the band gap of 270 compounds using PBE, mBJLDA, and G_0W_0 . They found experimental values for 32 of these compounds, and for this subset the root mean squared error is 1.77, 0.91, and 0.50 eV for PBE, mBJLDA, and G_0W_0 , respectively.

In Ref. 30, the performance of the GLLB-SC and mBJLDA potentials were compared on a set consisting of 33 chalcopyrite, kesterite, and wurtzite polymorphs of II-IV-V₂ and III-III-V₂ semiconductors. The GLLB-SC and mBJLDA band gaps are relatively close in the majority of cases. Since the experimental values are known for only half of the systems, a conclusion about the relative accuracy of GLLB-SC and mBJLDA was not really possible.

In a very recent study, Nakano and Sakai³¹ calculated the band gap, refractive index, and extinction coefficient of 70 solids with the PBE and mBJLDA methods. In this work, one of the parametrization of mBJLDA from Ref. 73 was used. Similarly as in the test set of 472 solids discussed in Sec. III A 2, the solids are of various types ranging from simple systems like diamond or BN to more complicated cases like LiTaO₃ or Y₃Al₅O₁₂. For the band gap, the root mean squared error with respect to experiment is 0.44 and 1.69 eV, for mBJLDA and PBE, respectively.

In Ref. 167, Meinert reported PBE and mBJLDA calculations on a set of 26 half-metallic Heusler compounds X_2YZ , where X and Y are 3d TM, and Z is a main group element. One of his conclusions is that mBJLDA gives too large band gaps, while PBE only slightly underestimates. However, as mentioned by Meinert, the experimental measurement of the half-metallic band gap is difficult and can only be made indi-

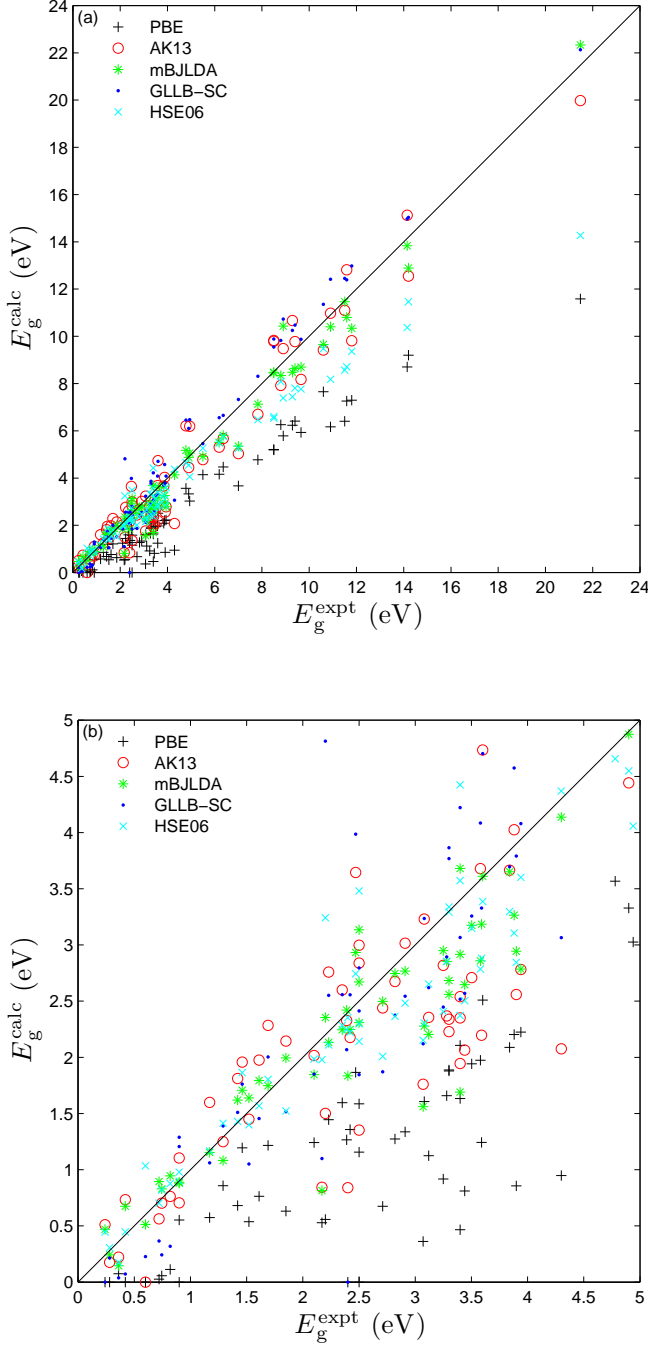


FIG. 2. Calculated versus experimental fundamental band gaps for the set of 76 solids. The values can be found in Refs. 29 and 32. The lower panel is a zoom of the upper panel focusing on band gaps smaller than 5 eV.

rectly. In addition, such experimental results were available only for a few of the systems.

On the side of the GLLB-SC potential, we mention Ref. 168, where a MAE of 0.5 eV was obtained for a set of about 30 oxides. GLLB-SC was then further used for the search of new efficient photoelectrochemical cells among several thousands of oxides.^{168–170}

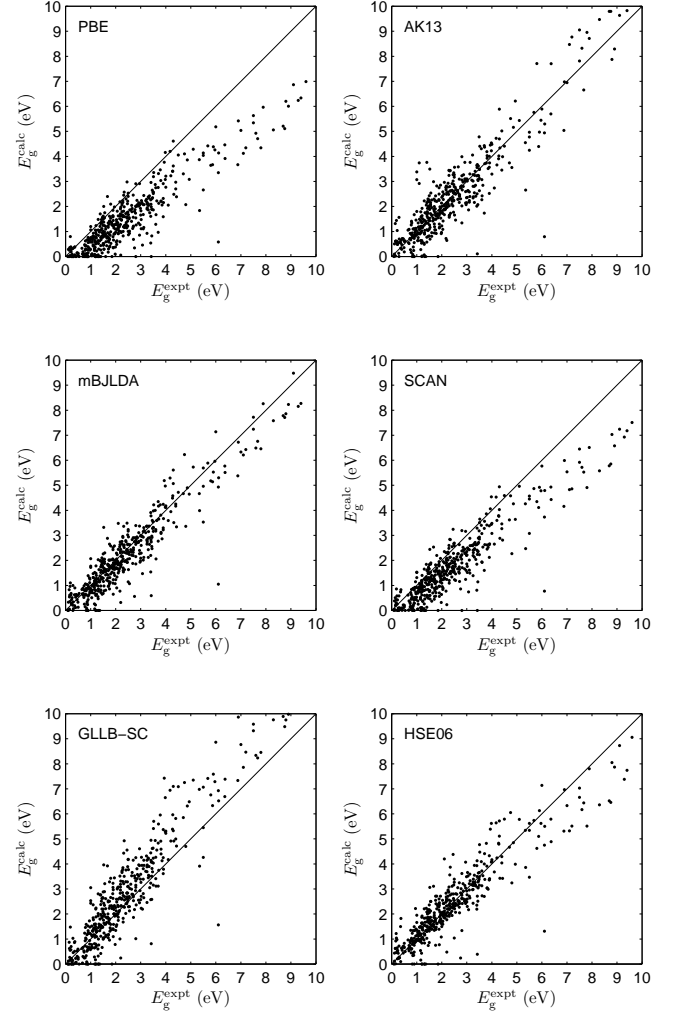


FIG. 3. Calculated versus experimental fundamental band gaps smaller than 10 eV for the set of 472 solids.³³

4. Further discussion

In conclusion, the results published so far have shown that among the computationally fast (i.e., semilocal) methods, the mBJLDA potential is overall the most accurate for band gap prediction. Other methods like the GLLB-SC potential or the MGGA HLE17 may reach similar accuracy for a particular class of systems. Actually, GLLB-SC performs better than mBJLDA for Cu^{1+} compounds. However, for the AFM TM solids, mBJLDA is clearly superior and reaches the accuracy of the much more expensive hybrid functionals. We mention that the more sophisticated hybrid methods with a fraction α_x of HF exchange that depends on the dielectric function seem to be more accurate than traditional hybrids and mBJLDA.³⁷

We should also mention that Jishi *et al.*⁷⁴ pointed out that, although improving over PBE, mBJLDA still underestimates the band gap in lead halide perovskites by roughly 1 eV when spin-orbit coupling is included in the calculation. They proposed a reparametrization [$\alpha = 0.4$ and $\beta = 1.0 \text{ bohr}^{1/2}$ in

TABLE III. Fundamental band gap (in eV) in rare-earth oxides (CeO_2 and Ce_2O_3) and one actinide oxide (UO_2). The results were obtained with the WIEN2K code.

	CeO_2	Ce_2O_3	UO_2
PBE	2.0	0.0	0.0
HLE16	1.4	0.2	0.0
mBJLDA	2.2	1.3	0.5
GLLB-SC	3.5	1.5	0.9
PBE+ U	2.5	2.3	2.9
Expt.	3 ^a	2.4 ^b	2.0 ^c

^a Ref. 171.

^b Ref. 172.

^c Ref. 173.

Eq. (16)] which leads to excellent agreement with experiment, but would lead to overestimations for other systems (see Sec. V). Similar observations were made in Ref. 75 about the more complicated layered hybrid organic-inorganic lead halide perovskites.

In the literature, not much has been said about the accuracy of specialized potentials like mBJLDA or GLLB-SC for systems with a $4f$ or $5f$ (open) shell at the VBM or CBM. In order to give a vague idea, we considered CeO_2 (non-magnetic), Ce_2O_3 (AFM), and UO_2 (AFM). The results obtained with the WIEN2K code for a few selected methods are shown in Table III, where in addition to the experimental values, PBE+ U results are also given. For all three systems, the PBE+ U calculations were done using the fully localized limit version¹⁷⁴ with $U = 5$ and $J = 0.5$ eV, which are similar to suggested values.^{175,176} For CeO_2 , mBJLDA (but not HLE16) slightly improves over PBE, while GLLB-SC widens further the band gap. For Ce_2O_3 and UO_2 , none of the methods except PBE+ U leads to reasonable band gaps. Furthermore, taking into account spin-orbit coupling for UO_2 (not done for the present work) should reduce further the calculated band gap. Overall, GLLB-SC is more accurate than PBE, HLE16, and mBJLDA, but less than PBE+ U , which should be the preferred fast method for $4f$ and $5f$ systems. Note that the hybrid functional HSE leads to good agreement with experiment for the three systems.^{176,177}

At that point we want to mention other fast DFT schemes for band gap calculations that we did not consider for the present work. A few of them do not consist of a particular xc potential, but of a post-KS-DFT procedure with standard LDA or PBE. The methods of Chan and Ceder¹⁷⁸ and Zheng *et al.*¹⁷⁹ lead to results similar to mBJLDA for typical sp -semiconductors, and actually more accurate for ZnO, which is a difficult case for mBJLDA. By making simplifications in the GW equations, Johnson and Ashcroft¹⁸⁰ proposed a shift for the conduction band. This is somehow in the same spirit as the GLLB-SC method, but with the disadvantage that the dielectric constant is needed.

B. Other properties

In Sec. IID, it was mentioned that multiplicative potentials like mBJLDA, AK13, or HLE16 leading to band gaps E_g^{KS} close to E_g may possibly lead to inaccurate results for other properties. Below, a short summary of the performance of xc potentials on properties other than the fundamental band gap is given.

1. Effective mass and bandwidth

In Refs. 32 and 181 (see also Ref. 182), the effective hole and electron masses were calculated for five III-V semiconductors (InP, InAs, InSb, GaAs, and GaSb). The results showed that HLE16 and mBJLDA increase very often, but not systematically, the effective masses compared to PBE. With both methods, the tendency is to yield values that are larger than experiment. Overall, the results^{32,181} with HLE16 and mBJLDA are more accurate than with the standard PBE, but less accurate than with the hybrid HSE (as shown recently in Ref. 183 for Ge) or EV93PW91. GLLB-SC was shown to be not particularly accurate for the III-V semiconductors.³² The overestimation of the effective mass by mBJLDA in various perovskites has been reported in recent works.^{75,184} In particular, in Ref. 75 a reoptimization of the α and β parameters in mBJLDA [Eq. (16)] specific for lead halide perovskites and within a pseudopotential implementation has been proposed (see also Refs. 74 and 185). It is shown that the overestimation of the reduced effective mass with the reoptimized mBJLDA is of similar magnitude as the underestimation with LDA.

As underlined, e.g., in Refs. 75, 76, 133, 182, 186–188, a narrowing of electronic bands is observed with mBJLDA compared to LDA/PBE, which is related to the increase in the effective mass observed above. On a set of ten cubic semiconductors and insulators, Waroquiers *et al.*¹³³ showed that mBJLDA clearly underestimates the bandwidth with respect to experiment and is less accurate than LDA. For this test set LDA is, on average, as accurate as G_0W_0 . Actually, the too narrow bands obtained with mBJLDA have recently been shown to be a source of problem for optical spectra in ZnSe.¹⁸⁸ A similar reduction in the bandwidth has been observed with the AK13 potential⁵⁰ and most likely the same problem occurs with HLE16.

In summary, while mBJLDA is much more accurate than the standard LDA and PBE for the fundamental band gap, it seems to be of similar accuracy as (or possibly slightly more accurate than) PBE for the effective mass, but quite inaccurate for the bandwidth.

2. Optics

The mBJLDA potential has also been used quite frequently for the calculation of the optical properties of solids. A few representative works reporting calculations of (non-)linear optics using the RPA for the dielectric function is given by

Refs. 31, 183, 187, 189–194. Without entering into details, a rather general conclusion from all these studies is that mBJLDA improves over LDA and PBE for the optical properties. This is not that surprising since an improvement in the band gap should in principle be followed by a more realistic onset in the absorption spectrum.

We also mention a series of studies from Yabana and co-workers (see, e.g., Refs. 195–200) who used mBJLDA within time-dependent DFT (TDDFT) to study nonlinear effects induced by strong short laser pulses. For instance, in Ref. 197 they showed that in Si and Ge, mBJLDA and HSE lead to very similar results (for the dielectric function and excitation energies) and improve over LDA. However, it was also noticed that special care is needed in order to get a stable time evolution in TDDFT when using the mBJLDA potential.¹⁹⁷ Similar problems with the original BJ potential were reported in Ref. 88.

Regarding other xc methods, Vlček *et al.*⁵⁰ reported an improvement (with respect to PBE) in the dielectric constant when using AK13. Calculations of the dielectric constant with TDDFT²⁰¹ showed that GLLB-SC degrades the results with respect to LDA, in particular if the derivative discontinuity is taken into account. However, these errors obtained with GLLB-SC were attributed to the missing electron-hole interaction in the calculation of the RPA (or adiabatic LDA) response function.

3. Magnetism

Concerning magnetism, it has been shown that the mBJLDA potential provides very accurate values of the atomic magnetic moment in AFM systems with localized electrons. In Refs. 20, 32, 227, and 228, we showed that mBJLDA increases by 0.2–0.4 μ_B the atomic spin moment μ_S with respect to PBE. Since PBE quasi-systematically underestimates μ_S in AFM systems, such an increase leads to better agreement with experiment. In Table IV, results from Ref. 32 for AFM TM oxides are reproduced for selected xc methods. Compared to PBE, all other methods lead to larger μ_S values. Since there is sometimes a rather large uncertainty in the experimental value and, furthermore, the orbital component μ_L is not known precisely, it is difficult to say which method is the best. Anyway, in most cases the agreement with experiment is much improved compared to PBE and satisfactory. We just note that HLE16 seems to underestimate (overestimate) the value in CuO (Cr₂O₃) and that GLLB-SC overestimates for Cr₂O₃ and Fe₂O₃. The advantage of these methods over DFT+ U ,¹⁹ which is widely used for AFM oxides, is that they do not contain a system-dependent parameter like U .

Table V shows the results for μ_S in the ferromagnetic metals Fe, Co, and Ni (results from Ref. 32). Unlike in AFM systems with localized electrons, the LDA and standard GGAs lead usually to reasonable values of the moment in itinerant metals. Indeed, PBE only slightly overestimates with respect to experiment, while the other methods clearly overestimate the values. For the three metals, GLLB-SC and HSE06 overestimate more than mBJLDA and HLE16. We mention that

the reverse has been observed by Singh⁷⁶ in the ferromagnetic metal Gd, a 4*f*-system, in which the mBJLDA moment is smaller than the PBE one and than the experimental value by $\sim 1 \mu_B$. Thus, contrary to what has been observed in 3*d* magnetic systems, the mBJLDA potential reduces the exchange splitting in Gd (due to an increase of occupancy of the minority 4*f* states) and shifts the *spd*-bands up with respect to the 4*f* bands.

In the work of Meinert¹⁶⁷ on half-metallic Heusler compounds already mentioned in Sec. III A 3, it is shown that the PBE and mBJLDA magnetic moments are the same in most cases, which is simply due to the half-metallic state. Only for Co₂FeSi and Co₂FeGe the moment is clearly different with mBJLDA (larger by $\sim 0.35 \mu_B$) and actually in better agreement with experiment.

Regarding the performance of MGGA functionals implemented with a non-multiplicative potential, a certain number of results are available for ferromagnetic metals.^{95,234–240} From these studies the most interesting results concern the SCAN functional, which has been shown to overestimate the magnetic moment, and sometimes by a rather large amount (e.g., $\sim 0.5 \mu_B$ for Fe). However, such overestimation is not systematically observed with functionals of this class, since other MGGA functionals like TPSS¹⁶³ or revTPSS¹⁶⁴ lead to values similar to PBE.^{95,234,239}

In summary, the standard LDA and GGA lead to magnetic moments which are qualitatively correct for itinerant metals, but not for AFM solids with strongly correlated electrons (strong underestimation). On the other hand, methods giving much more reasonable magnetic moments in AFM solids, e.g., mBJLDA, GLLB-SC, or HSE06, lead to strong overestimation in itinerant metals. However, it is important to note that the overestimation of the moment in Fe, Co, and Ni with mBJLDA is much less severe than with GLLB-SC and HSE06 (an explanation is provided in Sec. V). Note that the inadequacy of hybrid functionals for metals has been documented.^{241–244} Currently, there is no DFT method that is able to provide qualitatively correct values of the moment in itinerant metals and AFM solids simultaneously.

4. Electron density

The quality of the electron density ρ can be measured by considering the electric field gradient (EFG) or the X-ray structure factors. The EFG is defined as the second derivative of the Coulomb potential at a nucleus and, therefore, depends on the charge distribution in the solid. In Ref. 32, the calculated EFG of seven metals (Ti, Zn, Zr, Tc, Ru, Cd, and Cu₂Mg) and two non-metals (CuO and Cu₂O) has been calculated and compared to experiment. For some of the systems, the error bar on the experimental value is quite large, nevertheless it was possible to draw some conclusions on the accuracy of the methods. The method that is the most accurate overall is the GLLB-SC potential that leads to reasonable errors for all systems. The methods that were shown to be quite inaccurate are LDA, Sloc, HLE16, mBJLDA, and LB94.

In the same work,³² the calculated and experimental X-ray

TABLE IV. Atomic spin magnetic moment μ_S (in μ_B) of AFM TM oxides compared to the experimental total moment $\mu_S + \mu_L$. The orbital moment μ_L should be in the range 0.6-1 μ_B for FeO,^{106,202-204} 1-1.6 μ_B for CoO,^{106,202-211} 0.3-0.45 μ_B for NiO,^{202,203,207,210,212} and smaller for the other cases. The theoretical results, obtained with the WIEN2K code, are from Ref. 32.

Method	MnO	FeO	CoO	NiO	CuO	Cr ₂ O ₃	Fe ₂ O ₃
PBE	4.17	3.39	2.43	1.38	0.38	2.44	3.53
HLE16	4.51	3.62	2.59	1.48	0.40	2.96	4.02
mBJLDA	4.41	3.58	2.71	1.75	0.74	2.60	4.09
GLLB-SC	4.56	3.74	2.73	1.65	0.55	2.99	4.43
HSE06	4.36	3.55	2.65	1.68	0.67	2.61	4.08
Expt.	4.58 ^a	3.32, ^b 4.2, ^c 4.6 ^d	3.35, ^e 3.8, ^{bf} 3.98 ^g	1.9, ^{ab} 2.2 ^{hi}	0.65 ^j	2.44, ^k 2.48, ^l 2.76 ^m	4.17, ⁿ 4.22 ^o

^a Ref. 213.

^b Ref. 214.

^c Ref. 215.

^d Ref. 216.

^e Ref. 217.

^f Ref. 218.

^g Ref. 219.

^h Ref. 212.

ⁱ Ref. 220.

^j Ref. 221.

^k Ref. 222.

^l Ref. 223.

^m Ref. 224.

ⁿ Ref. 225.

^o Ref. 226.

TABLE V. Unit cell spin magnetic moment μ_S (in μ_B /atom) of 3d TM. The experimental values are also spin magnetic moments. The theoretical results, obtained with the WIEN2K code, are from Ref. 32.

Method	Fe	Co	Ni
PBE	2.22	1.62	0.64
HLE16	2.72	1.72	0.63
mBJLDA	2.51	1.69	0.73
GLLB-SC	3.08	1.98	0.81
HSE06	2.79	1.90	0.88
Expt.	1.98, ^a 2.05, ^b 2.08 ^c	1.52, ^c 1.58, ^{bd} 1.55-1.62 ^a	0.52, ^c 0.55 ^{be}

^a Ref. 229.

^b Ref. 230.

^c Ref. 231.

^d Ref. 232.

^e Ref. 233.

structure factors of Si were compared. The best method is the screened hybrid HSE06, followed by PBE, EV93PW91, and BJLDA. The mBJLDA potential is less accurate than these methods, but slightly more accurate than LDA. The Sloc and HLE16 were shown to be much more inaccurate than all other methods, while LB94 and GLLB-SC are also very inaccurate, but to a lesser extent. Actually, in the case of GLLB-SC it is the core density that is particularly badly described, while the valence density seems to be rather accurate (see Ref. 32 for details), which is consistent with the very good description of the EFG mentioned above.

In an interesting recent study,²⁴⁵ it was shown that functionals like SCAN or HSE06 which were constructed more from first-principles by using mathematical constraints rather than empirically by fitting a large number of coefficients pro-

duce more accurate electron density, however the test set consists only of atoms/cations with 2, 4, or 10 electrons. Highly parametrized functionals like those of the Minnesota family²⁴⁶ are much less accurate.

To finish this section, we mention a study on VO₂, where various functionals are compared for the electron density. Accurate electron densities from Monte-Carlo calculations were used as reference. It is shown that hybrid functionals like HSE are more accurate than LDA and PBE.

IV. SUMMARY

From the overview of the literature results presented in Sec. III, the main conclusions are the following:

- Among the semilocal methods, the mBJLDA potential is on average the most accurate for the fundamental band gap. Furthermore, mBJLDA is at least as accurate as hybrid functionals like HSE06. Only the most advanced methods, namely the dielectric-function-dependent hybrid functionals and *GW*, can be consistently more accurate than mBJLDA.
- A particularly strong advantage of mBJLDA over the other methods is its reliability for all kinds of systems. mBJLDA is more or less equally accurate for large band gap insulators (ionic solids, rare gases), *sp*-semiconductors, and systems with TM atoms including AFM systems with localized 3d-electrons.
- All other semilocal potentials are very unreliable for the band gap in AFM systems.

- The cases where mBJLDA is clearly not accurate enough are the Cu^{1+} compounds (for which GLLB-SC works much better), but also ZnO, where the band gap is still underestimated by at least 1 eV. Note that a modification of mBJLDA, called the universal correction,⁷¹ may help for Cu^{1+} compounds (see Ref. 55 for details). Lead halide perovskites require another set of parameters α and β in mBJLDA, while none of the multiplicative potentials leads to meaningful band gaps for the $4f$ and $5f$ systems.
- The bandwidth is not reproduced accurately by mBJLDA which makes the bands too narrow. LDA and PBE are more accurate than mBJLDA.
- The magnetism in AFM systems is very well described with mBJLDA and as accurately as with hybrid functionals. In ferromagnetic metals the magnetic moment is too large, however the overestimation is not as large as with GLLB-SC and hybrid functionals.
- The electron density does not seem to be particularly well described by mBJLDA. The standard PBE is more accurate, while HLE16 and GLLB-SC are extremely inaccurate. HSE06 is particularly good for the electron density of Si.
- Beside mBJLDA, DFT+ U is the only other computationally cheap method that is able to provide qualitatively correct results in AFM systems for the band gap and magnetic moment.

Thus, this summary shows that the mBJLDA potential is currently the best alternative to the much more expensive hybrid or GW methods. This explains why it has been implemented in various codes^{75,77,78,167,181,247–250} and used for numerous applications. Examples are the search for efficient thermoelectric materials,^{251–264} topological insulators,^{254,265–285} or materials for photovoltaics.^{23,286–288} The mBJLDA potential has also been used for the screening of materials or in relation to machine learning techniques^{28,289,290} (see Refs. 168–170, 291–293 for such works using the GLLB-SC potential). Furthermore, it has been shown to be accurate for the calculation of the ELNES (energy loss near-edge structure) spectrum of NiO ,²⁹⁴ and used recently for the band gap calculation of configurationally disordered semiconductors.²⁹⁵ Nevertheless, as a technical detail we should mention that the number of iterations to achieve self-consistent field convergence is usually (much) larger with the mBJLDA potential than with other potentials.

V. OUTLOOK

The question is why mBJLDA is more accurate than all other semilocal methods. The main reason is the use of two ingredients: the *kinetic-energy density* t_σ and the *average of $\nabla\rho/\rho$ in the unit cell* g [Eq. (17)], that are now discussed.

As illustrated and discussed in previous works,^{29,32,48} the mBJLDA potential is, compared to the PBE potential, more

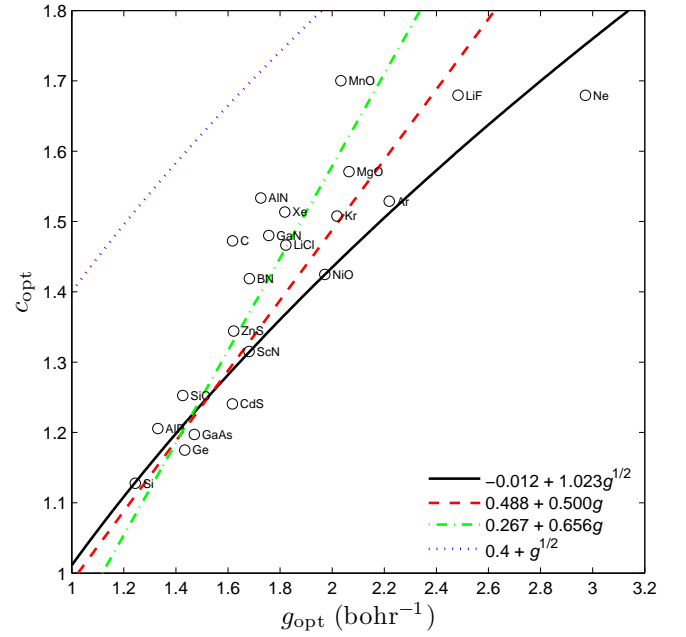


FIG. 4. Plot of c_{opt} versus g_{opt} (see text for explanations). The fit of these data points²⁰ given by Eq. (16) is represented by the solid curve. The two fits (of different sets of solids) proposed in Ref. 73 are represented by the dashed and dash-dotted curves, and the fit from Ref. 74 specific for lead halide perovskites is represented by the dotted curve.

negative around the nuclei (where the orbital of the VBM is usually located) and less negative in the interstitial region (where the orbital of the CBM is located). This enlarges the band gap. This mechanism, which works in most ionic solids and typical sp -semiconductors, is also used by the GGAs AK13, HLE16, and Sloc. However, these GGAs are not accurate for AFM systems, where the band gap may have a strong onsite $d-d$ character. In Ref. 227 it is shown that the second term in Eq. (15), which is proportional to $\sqrt{t_\sigma/\rho_\sigma}$, allows the potential to act differently on orbitals with different angular distributions (e.g., t_{2g} versus e_g of the $3d$ states) and increase a $d-d$ band gap. In order to do this, such a term in the mBJLDA potential is much more efficient than what GGA potentials can do. Actually, the t_σ -dependency in mBJLDA is strong, and most likely much stronger than in any other MGA like SCAN or HLE17, which are not as good as mBJLDA for AFM solids.

The integral given by Eq. (17), g , is even more crucial in explaining the success of the mBJLDA potential. Figure 4 shows a plot of c_{opt} versus g_{opt} , where c_{opt} is the value of c in Eq. (16) that would exactly lead to the experimental band gap and g_{opt} is the value of g obtained at the end of the self-consistent mBJLDA calculation done with c_{opt} . This is shown for all the solids, except two (FeO and ZnO), that were considered in our original work.²⁰ A correlation between c_{opt} and g_{opt} is clearly visible and the fit of these data that we chose in Ref. 20 is given by Eq. (16) with $\alpha = -0.012$ and $\beta = 1.023 \text{ bohr}^{1/2}$. Alternative fits⁷³ that were determined by using different sets of solids, e.g., focusing on small band

TABLE VI. Results obtained from mBJLDA calculations. Value of $g = g_{\text{SC}}$ [Eq. (17)] (in bohr^{-1}) obtained at the end of a usual self-consistent (SC) calculation. Fundamental band gap (in eV) and spin magnetic moment μ_S (in μ_B) obtained from a usual calculation ($g = g_{\text{SC}}$) or with g fixed ($g = g_{\text{fixed}}$) to the value obtained for the corresponding AFM oxide (for a metal) or metal (for a AFM oxide). The spin magnetic moment is the value in the unit cell and per atom for metals and inside the TM atomic sphere for the AFM oxides.

	Fe	Co	Ni	Cu	FeO	CoO	NiO	CuO
	1.40	1.48	1.54	g_{SC} 1.52	1.92	1.95	1.97	1.93
				Fundamental band gap				
With $g = g_{\text{SC}}$	0	0	0	0	1.84	3.14	4.14	2.27
With $g = g_{\text{fixed}}$	0	0	0	0	1.06	1.99	3.09	1.54
				μ_S				
With $g = g_{\text{SC}}$	2.51	3.38	0.73	0	3.58	2.71	1.75	0.74
With $g = g_{\text{fixed}}$	2.53	3.43	0.80	0	3.49	2.63	1.67	0.67

gaps are also shown. This rather clear correlation between c_{opt} and g_{opt} allows for a meaningful fit $c(g)$, which, when used in the mBJLDA potential, produces accurate band gaps. However, as mentioned in Sec. III, the standard parametrization of c is not good enough for lead halide perovskites, which require other values of α and β , and as shown in Fig. 4 this parametrization would lead to an overestimation of the band gap for other solids (in general, the band gap increases in a monotonous way with respect to c). Another illustration of the importance of g is given in Table VI, where the value of g for itinerant 3d TM and their oxides is shown. There is a clear difference between the metals and the oxides. While the value of g is in the range 1.40–1.54 bohr^{-1} for the metals, it is much larger, 1.92–1.97 bohr^{-1} , for the monoxides. From a more detailed analysis, we could see that this difference comes more particularly from the interstitial region, which is on average more inhomogeneous (larger $|\nabla\rho|/\rho$) for the oxides. However, also around the TM atom $|\nabla\rho|/\rho$ is larger for the oxides, which therefore also contributes in making g larger compared to the metal. If the calculation for the TM oxides is done by fixing the value of g in Eq. (16) to the value of the corresponding metal, then a large decrease of 0.7–1.1 eV in the band gap (and a large discrepancy with experiment) is obtained (Table VI). The same is observed for the magnetic moment, which is reduced in the oxides when the g of the metal is used. Conversely, using the value of g from the oxide for the calculation on the metals leads to an increase of the magnetic moment. The important point to note is that, in any case, using the incorrect g (i.e., the one from the other system) leads to much larger errors. We mention that other works using an average in the unit cell involving the density can be found in Refs. 34, 296–299.

However, since the mBJLDA potential is certainly not providing an optimal band gap in every case, and the results for other properties like the bandwidth or the electron density are even worse than with the standard PBE, there is room for improvement. As already mentioned in this work, forcing a multiplicative potential to give KS band gaps E_g^{KS} close to the experimental E_g is not really correct from the formal point of view and may result in a potential that is inappropriate for other properties. A derivative discontinuity Δ_{xc} should be present somewhere in the theory. Δ_{xc} is included

in the gKS band gap E_g^{gKS} with non-multiplicative potentials (MGGA and hybrid) or obtained from a post-KS calculation with the GLLB-SC potential.

Thus, from the discussion above, the strategy to follow for the construction of a *computationally fast* and *generally accurate* xc potential that alleviates the problems encountered with mBJLDA is quite obvious:

- The potential should be based on one of these two types: non-multiplicative MGGA or multiplicative of the GLLB-SC type. Then, a derivative discontinuity is available as it should be.
- Since both t_σ and g were shown to be crucial for the mBJLDA potential, most likely they can be useful for other types of potentials (by definition t_σ is used in a MGGA). Note that instead of g , a variant may be used, i.e., the average in the unit cell of a quantity different from $\nabla\rho/\rho$ may be more useful.

However, we mention that attempts (presented in Ref. 32 or unpublished) to improve over the GLLB-SC potential along these lines have been unsuccessful up to now. For instance, one of the most sophisticated variants of Eq. (18) that we have considered is of the form (the formula for Δ_x should be modified accordingly)

$$v_{\text{xc},\sigma}(\mathbf{r}) = cv_{\text{x},\sigma}^{\text{BR}}(\mathbf{r}) + (3c - 2)F_\sigma(\mathbf{r})K_x^{\text{LDA}} \times \sum_{n,\mathbf{k}} w_{n\mathbf{k}\sigma} \sqrt{\epsilon_{\text{H}} - \epsilon_{n\mathbf{k}\sigma}} \frac{|\psi_{n\mathbf{k}\sigma}(\mathbf{r})|^2}{\rho_\sigma(\mathbf{r})} + v_{\text{c},\sigma}^{\text{PBEsol}}(\mathbf{r}), \quad (28)$$

where F_σ is a function that depends on ρ_σ , $\nabla\rho_\sigma$, and t_σ and should satisfy $F_\sigma = 1$ for a constant electron density in order to recover the homogeneous electron gas limit, and c is a function that depends on some average in the unit cell similar to Eq. (16). With Eq. (28), that is of course inspired by the mBJLDA potential [Eq. (15)], we have not been able to find a strategy to parametrize c such that a clear correlation like in Fig. 4 for mBJLDA is obtained.

There are also a few drawbacks or challenges that should be mentioned:

- Modelizing a potential directly without requiring that it is a functional derivative is much easier and leads to much more flexibility. However, such stray potentials lead to problems^{59,68,88} and do not allow total-energy calculations. Thus, having a potential that is the derivative of a functional E_{xc} would be certainly much more interesting, but also much more challenging. AK13 and HLE16 satisfy this requirement, but the energy E_{xc} is very inaccurate.^{51,300,301}
- The use of the average in the unit cell of some quantity, e.g. g [Eq. (17)], works only in the case of bulk solids. Calculating such averages for systems with vacuum (surface or molecule) or interfaces makes no sense. Possible solutions to this problem have been proposed in Refs. 34 and 297 and consist of taking the average not over the unit cell, but over a region localized around the position \mathbf{r} where the potential is calculated. However, it is not clear how far such region should extend to bring enough nonlocal information.
- The use of the highest occupied and lowest unoccupied orbital energies like in the GLLB-SC potential [Eqs. (18) and (19)] is also problematic. For instance, the values of ϵ_H and ϵ_L for an interface correspond to one of the two bulk solids, while they correspond to the respective bulk solids when they are treated separately. This is somehow inconsistent. The solution would be to define position-dependent functions replacing ϵ_H and ϵ_L .

Trying to overcome these problems makes the search of a generally applicable xc potential even more difficult, however, as a first step they can be ignored.

SUPPLEMENTARY MATERIAL

See supplementary material for the detailed results for the band gap of the 472 solids discussed in Sec. III A 2.

ACKNOWLEDGMENTS

F.T., J.D., and P.B. acknowledge support from the Austrian Science Fund (FWF) through projects F41 (SFB Vi-CoM), P27738-N28, and W1243 (Solids4Fun). L.K. acknowledges support from the TU-D doctoral college (TU Wien). M.A.L.M. acknowledges partial support from the German DFG through the project MA6787/6-1.

¹W. Kohn and L. J. Sham, Phys. Rev. **140**, A1133 (1965).

²P. Hohenberg and W. Kohn, Phys. Rev. **136**, B864 (1964).

³L. Hedin, Phys. Rev. **139**, A796 (1965).

⁴F. Aryasetiawan and O. Gunnarsson, Rep. Prog. Phys. **61**, 237 (1998).

⁵X. Ren, P. Rinke, G. E. Scuseria, and M. Scheffler, Phys. Rev. B **88**, 035120 (2013).

⁶G. P. Chen, V. K. Voora, M. M. Agee, S. G. Balasubramani, and F. Furche, Annu. Rev. Phys. Chem. **68**, 421 (2017).

⁷S. Kümmel and L. Kronik, Rev. Mod. Phys. **80**, 3 (2008).

⁸A. J. Cohen, P. Mori-Sánchez, and W. Yang, Chem. Rev. **112**, 289 (2012).

⁹N. Mardirossian and M. Head-Gordon, Mol. Phys. **115**, 2315 (2017).

¹⁰S. Lehtola, C. Steigemann, M. J. T. Oliveira, and M. A. L. Marques, SoftwareX **7**, 1 (2018).

¹¹J. P. Perdew and K. Schmidt, AIP Conf. Proc. **577**, 1 (2001).

¹²J. P. Perdew, A. Ruzsinszky, J. Tao, V. N. Staroverov, G. E. Scuseria, and G. I. Csonka, J. Chem. Phys. **123**, 062201 (2005).

¹³J. P. Perdew, J. A. Chevary, S. H. Vosko, K. A. Jackson, M. R. Pederson, D. J. Singh, and C. Fiolhais, Phys. Rev. B **46**, 6671 (1992), **48**, 4978(E) (1993).

¹⁴J. P. Perdew, K. Burke, and M. Ernzerhof, Phys. Rev. Lett. **77**, 3865 (1996), **78**, 1396(E) (1997).

¹⁵J. Heyd, G. E. Scuseria, and M. Ernzerhof, J. Chem. Phys. **118**, 8207 (2003), **124**, 219906 (2006).

¹⁶Z. Wu and R. E. Cohen, Phys. Rev. B **73**, 235116 (2006).

¹⁷J. P. Perdew, A. Ruzsinszky, G. I. Csonka, O. A. Vydrov, G. E. Scuseria, L. A. Constantin, X. Zhou, and K. Burke, Phys. Rev. Lett. **100**, 136406 (2008), **102**, 039902(E) (2009).

¹⁸J. Sun, A. Ruzsinszky, and J. P. Perdew, Phys. Rev. Lett. **115**, 036402 (2015).

¹⁹V. I. Anisimov, J. Zaanen, and O. K. Andersen, Phys. Rev. B **44**, 943 (1991).

²⁰F. Tran and P. Blaha, Phys. Rev. Lett. **102**, 226401 (2009).

²¹M. Kuisma, J. Ojanen, J. Enkovaara, and T. T. Rantala, Phys. Rev. B **82**, 115106 (2010).

²²L. Yu and A. Zunger, Phys. Rev. Lett. **108**, 068701 (2012).

²³K. P. Ong, S. Wu, T. H. Nguyen, D. J. Singh, Z. Fan, M. B. Sullivan, and C. Dang, Sci. Rep. **9**, 2144 (2019).

²⁴Z. Xiao, R. A. Kerner, L. Zhao, N. L. Tran, K. M. Lee, T.-W. Koh, G. D. Scholes, and B. P. Rand, Nat. Phot. **11**, 108 (2017).

²⁵B. Mitchell, V. Dierolf, T. Gregorkiewicz, and Y. Fujiwara, J. Appl. Phys. **123**, 160901 (2018).

²⁶F. L. Traversa, F. Bonani, Y. V. Pershin, and M. Di Ventra, Nanotechnology **25**, 285201 (2014).

²⁷J. J. Urban, A. K. Menon, Z. Tian, A. Jain, and K. Hippalgaonkar, J. Appl. Phys. **125**, 180902 (2019).

²⁸J. Lee, A. Seko, K. Shitara, K. Nakayama, and I. Tanaka, Phys. Rev. B **93**, 115104 (2016).

²⁹F. Tran and P. Blaha, J. Phys. Chem. A **121**, 3318 (2017).

³⁰M. Pandey, K. Kuhar, and K. W. Jacobsen, J. Phys. Chem. C **121**, 17780 (2017).

³¹K. Nakano and T. Sakai, J. Appl. Phys. **123**, 015104 (2018).

³²F. Tran, S. Ehsan, and P. Blaha, Phys. Rev. Materials **2**, 023802 (2018).

³³P. Borlido, T. Aull, A. W. Huran, F. Tran, M. A. L. Marques, and S. Botti, J. Chem. Theory Comput. **15**, 5069 (2019).

³⁴M. A. L. Marques, J. Vidal, M. J. T. Oliveira, L. Reining, and S. Botti, Phys. Rev. B **83**, 035119 (2011).

³⁵D. Koller, P. Blaha, and F. Tran, J. Phys.: Condens. Matter **25**, 435503 (2013).

³⁶J. H. Skone, M. Govoni, and G. Galli, Phys. Rev. B **89**, 195112 (2014).

³⁷W. Chen, G. Miceli, G.-M. Rignanese, and A. Pasquarello, Phys. Rev. Materials **2**, 073803 (2018).

³⁸M. Shishkin, M. Marsman, and G. Kresse, Phys. Rev. Lett. **99**, 246403 (2007).

³⁹W. Chen and A. Pasquarello, Phys. Rev. B **92**, 041115(R) (2015).

⁴⁰A. Seidl, A. Görling, P. Vogl, J. A. Majewski, and M. Levy, Phys. Rev. B **53**, 3764 (1996).

⁴¹F. Della Sala, E. Fabiano, and L. A. Constantin, Int. J. Quantum Chem. **116**, 1641 (2016).

⁴²A. D. Becke, Phys. Rev. A **38**, 3098 (1988).

⁴³R. G. Parr and W. Yang, *Density-Functional Theory of Atoms and Molecules* (Oxford University Press, New York, 1989).

⁴⁴S. H. Vosko, L. Wilk, and M. Nusair, Can. J. Phys. **58**, 1200 (1980).

⁴⁵J. P. Perdew and Y. Wang, Phys. Rev. B **45**, 13244 (1992), **98**, 079904(E) (2018).

⁴⁶K. Finzel and A. I. Baranov, Int. J. Quantum Chem. **117**, 40 (2017).

⁴⁷E. Engel and S. H. Vosko, Phys. Rev. B **47**, 13164 (1993).

⁴⁸F. Tran, P. Blaha, and K. Schwarz, J. Phys.: Condens. Matter **19**, 196208 (2007).

⁴⁹R. Armiento and S. Kümmel, Phys. Rev. Lett. **111**, 036402 (2013).

- ⁵⁰V. Vlček, G. Steinle-Neumann, L. Leppert, R. Armiento, and S. Kümmel, *Phys. Rev. B* **91**, 035107 (2015).
- ⁵¹P. Verma and D. G. Truhlar, *J. Phys. Chem. Lett.* **8**, 380 (2017).
- ⁵²J. Heyd, J. E. Peralta, G. E. Scuseria, and R. L. Martin, *J. Chem. Phys.* **123**, 174101 (2005).
- ⁵³Á. Morales-García, R. Valero, and F. Illas, *J. Phys. Chem. C* **121**, 18862 (2017).
- ⁵⁴C. Lee, W. Yang, and R. G. Parr, *Phys. Rev. B* **37**, 785 (1988).
- ⁵⁵F. Tran, P. Blaha, M. Betzinger, and S. Blügel, *Phys. Rev. B* **91**, 165121 (2015).
- ⁵⁶M. Dion, H. Rydberg, E. Schröder, D. C. Langreth, and B. I. Lundqvist, *Phys. Rev. Lett.* **92**, 246401 (2004), **95**, 109902(E) (2005).
- ⁵⁷O. Gunnarsson, M. Jonson, and B. I. Lundqvist, *Solid State Commun.* **24**, 765 (1977).
- ⁵⁸J. A. Alonso and L. A. Girifalco, *Phys. Rev. B* **17**, 3735 (1978).
- ⁵⁹A. P. Gaiduk, S. K. Chulkov, and V. N. Staroverov, *J. Chem. Theory Comput.* **5**, 699 (2009).
- ⁶⁰R. van Leeuwen and E. J. Baerends, *Phys. Rev. A* **49**, 2421 (1994).
- ⁶¹P. R. T. Schipper, O. V. Gritsenko, S. J. A. van Gisbergen, and E. J. Baerends, *J. Chem. Phys.* **112**, 1344 (2000).
- ⁶²A. D. Becke and E. R. Johnson, *J. Chem. Phys.* **124**, 221101 (2006).
- ⁶³A. D. Becke and M. R. Roussel, *Phys. Rev. A* **39**, 3761 (1989).
- ⁶⁴F. Tran, P. Blaha, and K. Schwarz, *J. Chem. Theory Comput.* **11**, 4717 (2015).
- ⁶⁵J. C. Slater, *Phys. Rev.* **81**, 385 (1951).
- ⁶⁶A. P. Gaiduk and V. N. Staroverov, *J. Chem. Phys.* **128**, 204101 (2008).
- ⁶⁷V. N. Staroverov, *J. Chem. Phys.* **129**, 134103 (2008).
- ⁶⁸A. P. Gaiduk and V. N. Staroverov, *J. Chem. Phys.* **131**, 044107 (2009).
- ⁶⁹R. Armiento, S. Kümmel, and T. Körzdörfer, *Phys. Rev. B* **77**, 165106 (2008).
- ⁷⁰A. Karolewski, R. Armiento, and S. Kümmel, *J. Chem. Theory Comput.* **5**, 712 (2009).
- ⁷¹E. Räsänen, S. Pittalis, and C. R. Proetto, *J. Chem. Phys.* **132**, 044112 (2010).
- ⁷²S. Pittalis, E. Räsänen, and C. R. Proetto, *Phys. Rev. B* **81**, 115108 (2010).
- ⁷³D. Koller, F. Tran, and P. Blaha, *Phys. Rev. B* **85**, 155109 (2012).
- ⁷⁴R. A. Jishi, O. B. Ta, and A. A. Sharif, *J. Phys. Chem. C* **118**, 28344 (2014).
- ⁷⁵B. Traoré, G. Boudier, W. Lafargue-Dit-Hauret, X. Rocquefelte, C. Katan, F. Tran, and M. Kepenekian, *Phys. Rev. B* **99**, 035139 (2019).
- ⁷⁶D. J. Singh, *Phys. Rev. B* **82**, 205102 (2010).
- ⁷⁷A. P. Bartók and J. R. Yates, *Phys. Rev. B* **99**, 235103 (2019).
- ⁷⁸M. A. L. Marques, M. J. T. Oliveira, and T. Burnus, *Comput. Phys. Commun.* **183**, 2272 (2012).
- ⁷⁹O. Gritsenko, R. van Leeuwen, E. van Lenthe, and E. J. Baerends, *Phys. Rev. A* **51**, 1944 (1995).
- ⁸⁰E. J. Baerends, *Phys. Chem. Chem. Phys.* **19**, 15639 (2017).
- ⁸¹A. Lembarki, F. Rogemond, and H. Chermette, *Phys. Rev. A* **52**, 3704 (1995).
- ⁸²M. K. Harbola and K. D. Sen, *J. Phys. B: At. Mol. Phys.* **35**, 4711 (2002).
- ⁸³N. Umezawa, *Phys. Rev. A* **74**, 032505 (2006).
- ⁸⁴E. Fermi and E. Amaldi, *Accad. Ital. Rome* **6**, 117 (1934).
- ⁸⁵L. G. Ferreira, M. Marques, and L. K. Teles, *Phys. Rev. B* **78**, 125116 (2008).
- ⁸⁶K.-H. Xue, J.-H. Yuan, L. R. C. Fonseca, and X.-S. Miao, *Comput. Mater. Sci.* **153**, 493 (2018).
- ⁸⁷J. Doumont, F. Tran, and P. Blaha, *Phys. Rev. B* **99**, 115101 (2019).
- ⁸⁸A. Karolewski, R. Armiento, and S. Kümmel, *Phys. Rev. A* **88**, 052519 (2013).
- ⁸⁹T. Aschebrock, R. Armiento, and S. Kümmel, *Phys. Rev. B* **95**, 245118 (2017).
- ⁹⁰T. Aschebrock, R. Armiento, and S. Kümmel, *Phys. Rev. B* **96**, 075140 (2017).
- ⁹¹R. Neumann, R. H. Nobes, and N. C. Handy, *Mol. Phys.* **87**, 1 (1996).
- ⁹²A. V. Arbuznikov and M. Kaupp, *Chem. Phys. Lett.* **381**, 495 (2003).
- ⁹³J. Sun, J. P. Perdew, and A. Ruzsinszky, *Proc. Natl. Acad. Sci. U.S.A.* **112**, 685 (2015).
- ⁹⁴Z.-h. Yang, H. Peng, J. Sun, and J. P. Perdew, *Phys. Rev. B* **93**, 205205 (2016).
- ⁹⁵S. Jana, A. Patra, and P. Samal, *J. Chem. Phys.* **149**, 044120 (2018).
- ⁹⁶P. Verma and D. G. Truhlar, *J. Phys. Chem. C* **121**, 7144 (2017).
- ⁹⁷Y. Wang, X. Jin, H. S. Yu, D. G. Truhlar, and X. He, *Proc. Natl. Acad. Sci. U.S.A.* **114**, 8487 (2017).
- ⁹⁸D. M. Bylander and L. Kleinman, *Phys. Rev. B* **41**, 7868 (1990).
- ⁹⁹A. Alkauskas and A. Pasquarello, *Physica B* **401-402**, 670 (2007).
- ¹⁰⁰F. Tran, *Phys. Lett. A* **376**, 879 (2012).
- ¹⁰¹A. V. Krukau, O. A. Vydrov, A. F. Izmaylov, and G. E. Scuseria, *J. Chem. Phys.* **125**, 224106 (2006).
- ¹⁰²A. D. Becke, *J. Chem. Phys.* **98**, 5648 (1993).
- ¹⁰³J. M. Crowley, J. Tahir-Kheli, and W. A. Goddard, III, *J. Phys. Chem. Lett.* **7**, 1198 (2016).
- ¹⁰⁴J. P. Perdew and A. Zunger, *Phys. Rev. B* **23**, 5048 (1981).
- ¹⁰⁵P. Novák, J. Kuneš, L. Chaput, and W. E. Pickett, *Phys. Status Solidi B* **243**, 563 (2006).
- ¹⁰⁶F. Tran, P. Blaha, K. Schwarz, and P. Novák, *Phys. Rev. B* **74**, 155108 (2006).
- ¹⁰⁷R. T. Sharp and G. K. Horton, *Phys. Rev.* **90**, 317 (1953).
- ¹⁰⁸J. D. Talman and W. F. Shadwick, *Phys. Rev. A* **14**, 36 (1976).
- ¹⁰⁹E. Engel and R. M. Dreizler, *Density Functional Theory: An Advanced Course* (Springer, Berlin, 2011).
- ¹¹⁰M. Betzinger, C. Friedrich, A. Görling, and S. Blügel, *Phys. Rev. B* **85**, 245124 (2012).
- ¹¹¹D. Mejía-Rodríguez and S. B. Trickey, *Phys. Rev. A* **96**, 052512 (2017).
- ¹¹²D. Mejía-Rodríguez and S. B. Trickey, *Phys. Rev. B* **98**, 115161 (2018).
- ¹¹³A. V. Bienvenu and G. Knizia, *J. Chem. Theory Comput.* **14**, 1297 (2018).
- ¹¹⁴F. Tran, P. Kovács, L. Kalantari, G. K. H. Madsen, and P. Blaha, *J. Chem. Phys.* **149**, 144105 (2018).
- ¹¹⁵A. Alkauskas, P. Broqvist, F. Devynck, and A. Pasquarello, *Phys. Rev. Lett.* **101**, 106802 (2008).
- ¹¹⁶T. Shimazaki and Y. Asai, *Chem. Phys. Lett.* **466**, 91 (2008).
- ¹¹⁷M. Gerosa, C. E. Bottani, L. Caramella, G. Onida, C. Di Valentin, and G. Pacchioni, *Phys. Rev. B* **91**, 155201 (2015).
- ¹¹⁸Z.-H. Cui, Y.-C. Wang, M.-Y. Zhang, X. Xu, and H. Jiang, *J. Phys. Chem. Lett.* **9**, 2338 (2018).
- ¹¹⁹J. P. Perdew, R. G. Parr, M. Levy, and J. L. Balduz, Jr., *Phys. Rev. Lett.* **49**, 1691 (1982).
- ¹²⁰L. J. Sham and M. Schlüter, *Phys. Rev. Lett.* **51**, 1888 (1983).
- ¹²¹M. Levy, J. P. Perdew, and V. Sahni, *Phys. Rev. A* **30**, 2745 (1984).
- ¹²²M. Grüning, A. Marini, and A. Rubio, *J. Chem. Phys.* **124**, 154108 (2006).
- ¹²³M. Grüning, A. Marini, and A. Rubio, *Phys. Rev. B* **74**, 161103(R) (2006).
- ¹²⁴J. Klimeš and G. Kresse, *J. Chem. Phys.* **140**, 054516 (2014).
- ¹²⁵W. Yang, A. J. Cohen, and P. Mori-Sánchez, *J. Chem. Phys.* **136**, 204111 (2012).
- ¹²⁶J. P. Perdew, W. Yang, K. Burke, Z. Yang, E. K. U. Gross, M. Scheffler, G. E. Scuseria, T. M. Henderson, I. Y. Zhang, A. Ruzsinszky, H. Peng, J. Sun, E. Trushin, and A. Görling, *Proc. Natl. Acad. Sci. U.S.A.* **114**, 2801 (2017).
- ¹²⁷E. J. Baerends, *J. Chem. Phys.* **149**, 054105 (2018).
- ¹²⁸X. Andrade and A. Aspuru-Guzik, *Phys. Rev. Lett.* **107**, 183002 (2011).
- ¹²⁹J.-D. Chai and P.-T. Chen, *Phys. Rev. Lett.* **110**, 033002 (2013).
- ¹³⁰E. Kraisler and L. Kronik, *J. Chem. Phys.* **140**, 18A540 (2014).
- ¹³¹A. Görling, *Phys. Rev. B* **91**, 245120 (2015).
- ¹³²F. G. Eich and M. Hellgren, *J. Chem. Phys.* **141**, 224107 (2014).
- ¹³³D. Waroquiers, A. Lherbier, A. Miglio, M. Stankovski, S. Poncé, M. J. T. Oliveira, M. Giantomassi, G.-M. Rignanese, and X. Gonze, *Phys. Rev. B* **87**, 075121 (2013).
- ¹³⁴M. Govoni and G. Galli, *J. Chem. Theory Comput.* **11**, 2680 (2015).
- ¹³⁵W. Gao, W. Xia, X. Gao, and P. Zhang, *Sci. Rep.* **6**, 36849 (2016).
- ¹³⁶P. Liu, M. Kaltak, J. Klimeš, and G. Kresse, *Phys. Rev. B* **94**, 165109 (2016).
- ¹³⁷H. Jiang, R. I. Gomez-Abal, P. Rinke, and M. Scheffler, *Phys. Rev. B* **82**, 045108 (2010).
- ¹³⁸B.-C. Shih, Y. Xue, P. Zhang, M. L. Cohen, and S. G. Louie, *Phys. Rev. Lett.* **105**, 146401 (2010).
- ¹³⁹C. Friedrich, M. C. Müller, and S. Blügel, *Phys. Rev. B* **83**, 081101(R) (2011), **84**, 039906 (2011).
- ¹⁴⁰H. Jiang and P. Blaha, *Phys. Rev. B* **93**, 115203 (2016).
- ¹⁴¹Z. Zhu and U. Schwingenschlögl, *Phys. Rev. B* **86**, 075149 (2012).
- ¹⁴²P. Blaha, K. Schwarz, G. K. H. Madsen, D. Kvasnicka, J. Luitz, R. Laskowski, F. Tran, and L. D. Marks, *WIEN2k: An Augmented Plane*

- Wave plus Local Orbitals Program for Calculating Crystal Properties* (Vienna University of Technology, Austria, 2018).
- ¹⁴³D. J. Singh and L. Nordström, *Planewaves, Pseudopotentials, and the LAPW Method, 2nd ed.* (Springer, New York, 2006).
 - ¹⁴⁴F. Tran and P. Blaha, *Phys. Rev. B* **83**, 235118 (2011).
 - ¹⁴⁵M. J. Lucero, T. M. Henderson, and G. E. Scuseria, *J. Phys.: Condens. Matter* **24**, 145504 (2012).
 - ¹⁴⁶S. Bernstorff and V. Saile, *Opt. Commun.* **58**, 181 (1986).
 - ¹⁴⁷R. Gillen and J. Robertson, *J. Phys.: Condens. Matter* **25**, 165502 (2013).
 - ¹⁴⁸L. Schimka, J. Harl, and G. Kresse, *J. Chem. Phys.* **134**, 024116 (2011).
 - ¹⁴⁹H. Shi, R. I. Eglitis, and G. Borstel, *Phys. Rev. B* **72**, 045109 (2005).
 - ¹⁵⁰A. M. Ganose and D. O. Scanlon, *J. Mater. Chem. C* **4**, 1467 (2016).
 - ¹⁵¹D. Groh, R. Pandey, M. B. Sahariah, E. Amzallag, I. Baraille, and M. Rérat, *J. Phys. Chem. Solids* **70**, 789 (2009).
 - ¹⁵²V. Eyert, *Phys. Rev. Lett.* **107**, 016401 (2011).
 - ¹⁵³P. E. Blöchl, *Phys. Rev. B* **50**, 17953 (1994).
 - ¹⁵⁴G. Kresse and J. Furthmüller, *Phys. Rev. B* **54**, 11169 (1996).
 - ¹⁵⁵Y. Zhao and D. G. Truhlar, *J. Chem. Phys.* **130**, 074103 (2009).
 - ¹⁵⁶R. Peverati and D. G. Truhlar, *J. Chem. Theory Comput.* **8**, 2310 (2012).
 - ¹⁵⁷R. Peverati and D. G. Truhlar, *J. Chem. Phys.* **136**, 134704 (2012).
 - ¹⁵⁸R. Peverati and D. G. Truhlar, *Phys. Chem. Chem. Phys.* **14**, 13171 (2012).
 - ¹⁵⁹B. Xiao, J. Sun, A. Ruzsinszky, J. Feng, R. Haunschild, G. E. Scuseria, and J. P. Perdew, *Phys. Rev. B* **88**, 184103 (2013).
 - ¹⁶⁰Y. Mo, G. Tian, and J. Tao, *Chem. Phys. Lett.* **682**, 38 (2017).
 - ¹⁶¹B. Patra, S. Jana, L. A. Constantin, and P. Samal, *Phys. Rev. B* **100**, 045147 (2019).
 - ¹⁶²H. Peng and J. P. Perdew, *Phys. Rev. B* **96**, 100101(R) (2017).
 - ¹⁶³J. Tao, J. P. Perdew, V. N. Staroverov, and G. E. Scuseria, *Phys. Rev. Lett.* **91**, 146401 (2003).
 - ¹⁶⁴J. P. Perdew, A. Ruzsinszky, G. I. Csonka, L. A. Constantin, and J. Sun, *Phys. Rev. Lett.* **103**, 026403 (2009), **106**, 179902 (2011).
 - ¹⁶⁵J. Tao and Y. Mo, *Phys. Rev. Lett.* **117**, 073001 (2016).
 - ¹⁶⁶H. Jiang, *J. Chem. Phys.* **138**, 134115 (2013).
 - ¹⁶⁷M. Meinert, *Phys. Rev. B* **87**, 045103 (2013).
 - ¹⁶⁸I. E. Castelli, T. Olsen, S. Datta, D. D. Landis, S. Dahl, K. S. Thygesen, and K. W. Jacobsen, *Energy Environ. Sci.* **5**, 5814 (2012).
 - ¹⁶⁹I. E. Castelli, D. D. Landis, K. S. Thygesen, S. Dahl, I. Chorkendorff, T. F. Jaramillo, and K. W. Jacobsen, *Energy Environ. Sci.* **5**, 9034 (2012).
 - ¹⁷⁰I. E. Castelli, F. Hüser, M. Pandey, H. Li, K. S. Thygesen, B. Seger, A. Jain, K. A. Persson, G. Ceder, and K. W. Jacobsen, *Adv. Energy Mater.* **5**, 1400915 (2014).
 - ¹⁷¹E. Wuilloud, B. Delley, W.-D. Schneider, and Y. Baer, *Phys. Rev. Lett.* **53**, 202 (1984).
 - ¹⁷²A. V. Prokofiev, A. I. Shelykh, and B. T. Melekh, *J. Alloys Compd.* **242**, 41 (1996).
 - ¹⁷³H. Idriss, *Surf. Sci. Rep.* **65**, 67 (2010).
 - ¹⁷⁴M. T. Czyżyk and G. A. Sawatzky, *Phys. Rev. B* **49**, 14211 (1994).
 - ¹⁷⁵J. L. F. Da Silva, M. V. Ganduglia-Pirovano, J. Sauer, V. Bayer, and G. Kresse, *Phys. Rev. B* **75**, 045121 (2007).
 - ¹⁷⁶H. He, D. A. Andersson, D. D. Allred, and K. D. Rector, *J. Phys. Chem. C* **117**, 16540 (2013).
 - ¹⁷⁷P. J. Hay, R. L. Martin, J. Uddin, and G. E. Scuseria, *J. Chem. Phys.* **125**, 034712 (2006).
 - ¹⁷⁸M. K. Y. Chan and G. Ceder, *Phys. Rev. Lett.* **105**, 196403 (2010).
 - ¹⁷⁹X. Zheng, A. J. Cohen, P. Mori-Sánchez, X. Hu, and W. Yang, *Phys. Rev. Lett.* **107**, 026403 (2011).
 - ¹⁸⁰K. A. Johnson and N. W. Ashcroft, *Phys. Rev. B* **58**, 15548 (1998).
 - ¹⁸¹Y.-S. Kim, M. Marsman, G. Kresse, F. Tran, and P. Blaha, *Phys. Rev. B* **82**, 205212 (2010).
 - ¹⁸²R. B. Araujo, J. S. de Almeida, and A. Ferreira da Silva, *J. Appl. Phys.* **114**, 183702 (2013).
 - ¹⁸³C. Rödl, J. Furthmüller, J. R. Suckert, V. Armuzza, F. Bechstedt, and S. Botti, *Phys. Rev. Materials* **3**, 034602 (2019).
 - ¹⁸⁴I. Ohkubo and T. Mori, *J. Phys. Soc. Jpn.* **86**, 074705 (2017).
 - ¹⁸⁵R. A. Jishi, *AIMS Mater. Sci.* **3**, 149 (2016).
 - ¹⁸⁶P. V. Smith, M. Hermanowicz, G. A. Shah, and M. W. Radny, *Comput. Mater. Sci.* **54**, 37 (2012).
 - ¹⁸⁷G. Kresse, M. Marsman, L. E. Hintzschke, and E. Flage-Larsen, *Phys. Rev. B* **85**, 045205 (2012).
 - ¹⁸⁸C.-Y. Wang, P. Elliott, S. Sharma, and J. K. Dewhurst, *J. Phys.: Condens. Matter* **31**, 214002 (2019).
 - ¹⁸⁹D. J. Singh, *Phys. Rev. B* **82**, 155145 (2010).
 - ¹⁹⁰F. Karsai, P. Tiwald, R. Laskowski, F. Tran, D. Koller, S. Gräfe, J. Burgdörfer, L. Wirtz, and P. Blaha, *Phys. Rev. B* **89**, 125429 (2014).
 - ¹⁹¹A. H. Reshak, *J. Appl. Phys.* **119**, 105706 (2016).
 - ¹⁹²J. Kopaczek, M. P. Polak, P. Scharoch, K. Wu, B. Chen, S. Tongay, and R. Kudrawiec, *J. Appl. Phys.* **119**, 235705 (2016).
 - ¹⁹³P. Ondračka, D. Holec, D. Nečas, E. Kedroňová, S. Elisabeth, A. Goullet, and L. Zajíčková, *Phys. Rev. B* **95**, 195163 (2017).
 - ¹⁹⁴W. Ibarra-Hernández, H. Elsayed, A. H. Romero, A. Bautista-Hernández, D. Olguín, and A. Cantarero, *Phys. Rev. B* **96**, 035201 (2017).
 - ¹⁹⁵G. Wachter, C. Lemell, J. Burgdörfer, S. A. Sato, X.-M. Tong, and K. Yabana, *Phys. Rev. Lett.* **113**, 087401 (2014).
 - ¹⁹⁶S. A. Sato, K. Yabana, Y. Shinohara, T. Otobe, K.-M. Lee, and G. F. Bertsch, *Phys. Rev. B* **92**, 205413 (2015).
 - ¹⁹⁷S. A. Sato, Y. Taniguchi, Y. Shinohara, and K. Yabana, *J. Chem. Phys.* **143**, 224116 (2015).
 - ¹⁹⁸G. Wachter, S. A. Sato, I. Floss, C. Lemell, X.-M. Tong, K. Yabana, and J. Burgdörfer, *New J. Phys.* **17**, 123026 (2015).
 - ¹⁹⁹M. Uemoto, Y. Kuwabara, S. A. Sato, and K. Yabana, *J. Chem. Phys.* **150**, 094101 (2019).
 - ²⁰⁰A. Yamada and K. Yabana, *Eur. Phys. J. D* **73**, 87 (2019).
 - ²⁰¹J. Yan, K. W. Jacobsen, and K. S. Thygesen, *Phys. Rev. B* **86**, 045208 (2012).
 - ²⁰²A. Svane and O. Gunnarsson, *Phys. Rev. Lett.* **65**, 1148 (1990).
 - ²⁰³R. J. Radwanski and Z. Ropka, *Physica B* **403**, 1453 (2008).
 - ²⁰⁴A. Schrön and F. Bechstedt, *J. Phys.: Condens. Matter* **25**, 486002 (2013).
 - ²⁰⁵I. V. Solov'yev, A. I. Liechtenstein, and K. Terakura, *Phys. Rev. Lett.* **80**, 5758 (1998).
 - ²⁰⁶T. Shishidou and T. Jo, *J. Phys. Soc. Jpn.* **67**, 2637 (1998).
 - ²⁰⁷W. Neubeck, C. Vettier, F. de Bergevin, F. Yakhov, D. Mannix, L. Ranno, and T. Chatterji, *J. Phys. Chem. Solids* **62**, 2173 (2001).
 - ²⁰⁸W. Jauch and M. Reehuis, *Phys. Rev. B* **65**, 125111 (2002).
 - ²⁰⁹G. Ghiringhelli, L. H. Tjeng, A. Tanaka, O. Tjernberg, T. Mizokawa, J. L. de Boer, and N. B. Brookes, *Phys. Rev. B* **66**, 075101 (2002).
 - ²¹⁰R. J. Radwanski and Z. Ropka, *Physica B* **345**, 107 (2004).
 - ²¹¹A. Bousendel, N. Baadji, A. Haroun, H. Dreyssé, and M. Alouani, *Phys. Rev. B* **81**, 184432 (2010).
 - ²¹²V. Fernandez, C. Vettier, F. de Bergevin, C. Giles, and W. Neubeck, *Phys. Rev. B* **57**, 7870 (1998).
 - ²¹³A. K. Cheetham and D. A. O. Hope, *Phys. Rev. B* **27**, 6964 (1983).
 - ²¹⁴W. L. Roth, *Phys. Rev.* **110**, 1333 (1958).
 - ²¹⁵P. D. Battle and A. K. Cheetham, *J. Phys. C: Solid State Phys.* **12**, 337 (1979).
 - ²¹⁶H. Fjellvåg, F. Grønvald, S. Stølen, and B. Hauback, *J. Solid State Chem.* **124**, 52 (1996).
 - ²¹⁷D. C. Khan and R. A. Erickson, *Phys. Rev. B* **1**, 2243 (1970).
 - ²¹⁸D. Herrmann-Ronzau, P. Burlet, and J. Rossat-Mignod, *J. Phys. C: Solid State Phys.* **11**, 2123 (1978).
 - ²¹⁹W. Jauch, M. Reehuis, H. J. Bleif, F. Kubanek, and P. Pattison, *Phys. Rev. B* **64**, 052102 (2001).
 - ²²⁰W. Neubeck, C. Vettier, V. Fernandez, F. de Bergevin, and C. Giles, *J. Appl. Phys.* **85**, 4847 (1999).
 - ²²¹J. B. Forsyth, P. J. Brown, and B. M. Wanklyn, *J. Phys. C: Solid State Phys.* **21**, 2917 (1988).
 - ²²²N. O. Golosova, D. P. Kozlenko, S. E. Kichanov, E. V. Lukin, H.-P. Liermann, K. V. Glazyrin, and B. N. Savenko, *J. Alloys Compd.* **722**, 593 (2017).
 - ²²³P. J. Brown, J. B. Forsyth, E. Lelièvre-Berna, and F. Tasset, *J. Phys.: Condens. Matter* **14**, 1957 (2002).
 - ²²⁴L. M. Corliss, J. M. Hastings, R. Nathans, and G. Shirane, *J. Appl. Phys.* **36**, 1099 (1965).
 - ²²⁵V. Baron, J. Gutzmer, H. Rundlöf, and R. Tellgren, *Solid State Sci.* **7**, 753 (2005).
 - ²²⁶A. H. Hill, F. Jiao, P. G. Bruce, A. Harrison, W. Kockelmann, and C. Ritter, *Chem. Mater.* **20**, 4891 (2008).
 - ²²⁷D. Koller, F. Tran, and P. Blaha, *Phys. Rev. B* **83**, 195134 (2011).
 - ²²⁸A. S. Botana, F. Tran, V. Pardo, D. Baldomir, and P. Blaha, *Phys. Rev. B* **85**, 235118 (2012).

- ²²⁹C. T. Chen, Y. U. Idzerda, H.-J. Lin, N. V. Smith, G. Meigs, E. Chaban, G. H. Ho, E. Pellegrin, and F. Sette, *Phys. Rev. Lett.* **75**, 152 (1995).
- ²³⁰A. Scherz, Ph.D. thesis, Free University of Berlin (2003).
- ²³¹R. A. Reck and D. L. Fry, *Phys. Rev.* **184**, 492 (1969).
- ²³²R. M. Moon, *Phys. Rev.* **136**, A195 (1964).
- ²³³H. A. Mook, *J. Appl. Phys.* **37**, 1034 (1966).
- ²³⁴J. Sun, M. Marsman, G. I. Csonka, A. Ruzsinszky, P. Hao, Y.-S. Kim, G. Kresse, and J. P. Perdew, *Phys. Rev. B* **84**, 035117 (2011).
- ²³⁵E. B. Isaacs and C. Wolverton, *Phys. Rev. Materials* **2**, 063801 (2018).
- ²³⁶A. H. Romero and M. J. Verstraete, *Eur. Phys. J. B* **91**, 193 (2018).
- ²³⁷M. Ekholm, D. Gambino, H. J. M. Jönsson, F. Tasnádi, B. Alling, and I. A. Abrikosov, *Phys. Rev. B* **98**, 094413 (2018).
- ²³⁸Y. Fu and D. J. Singh, *Phys. Rev. Lett.* **121**, 207201 (2018).
- ²³⁹Y. Fu and D. J. Singh, *Phys. Rev. B* **100**, 045126 (2019).
- ²⁴⁰D. Mejía-Rodríguez and S. B. Trickey, *Phys. Rev. B* **100**, 041113(R) (2019).
- ²⁴¹J. Paier, M. Marsman, K. Hummer, G. Kresse, I. C. Gerber, and J. G. Ángyán, *J. Chem. Phys.* **124**, 154709 (2006), **125**, 249901 (2006).
- ²⁴²F. Tran, D. Koller, and P. Blaha, *Phys. Rev. B* **86**, 134406 (2012).
- ²⁴³Y.-R. Jang and B. D. Yu, *J. Phys. Soc. Jpn.* **81**, 114715 (2012).
- ²⁴⁴W. Gao, T. A. Abtew, T. Cai, Y.-Y. Sun, S. Zhang, and P. Zhang, *Solid State Commun.* **234-235**, 10 (2016).
- ²⁴⁵M. G. Medvedev, I. S. Bushmarinov, J. Sun, J. P. Perdew, and K. A. Lyssenko, *Science* **355**, 49 (2017).
- ²⁴⁶Y. Zhao and D. G. Truhlar, *Theor. Chem. Acc.* **120**, 215 (2008).
- ²⁴⁷M. César, Y. Ke, W. Ji, H. Guo, and Z. Mi, *Appl. Phys. Lett.* **98**, 202107 (2011).
- ²⁴⁸E. Germaneau, G. Su, and Q.-R. Zheng, *Comput. Phys. Commun.* **184**, 1697 (2013).
- ²⁴⁹L.-H. Ye, *Phys. Rev. B* **91**, 075101 (2015).
- ²⁵⁰S. Smidstrup, T. Markussen, P. Vancraeyveld, J. Wellendorff, J. Schneider, T. Gunst, B. Verstichel, D. Stradi, P. A. Khomyakov, U. G. Vej-Hansen, M.-E. Lee, S. T. Chill, F. Rasmussen, G. Penazzi, F. Corsetti, A. Ojanperä, K. Jensen, M. L. N. Palsgaard, U. Martinez, A. Blom, M. Brandbyge, and K. Stokbro, *arXiv e-prints*, arXiv:1905.02794 (2019).
- ²⁵¹D. Parker and D. J. Singh, *Phys. Rev. B* **85**, 125209 (2012).
- ²⁵²D. Parker, X. Chen, and D. J. Singh, *Phys. Rev. Lett.* **110**, 146601 (2013).
- ²⁵³V. Pardo, A. S. Botana, and D. Baldomir, *Phys. Rev. B* **87**, 125148 (2013).
- ²⁵⁴H. Shi, D. Parker, M.-H. Du, and D. J. Singh, *Phys. Rev. Applied* **3**, 014004 (2015).
- ²⁵⁵J. Zhang, L. Song, G. K. H. Madsen, K. F. F. Fischer, W. Zhang, X. Shi, and B. B. Iversen, *Nat. Commun.* **7**, 10892 (2016).
- ²⁵⁶G. Xing, J. Sun, Y. Li, X. Fan, W. Zheng, and D. J. Singh, *Phys. Rev. Materials* **1**, 065405 (2017), **1**, 079901 (2017).
- ²⁵⁷C.-J. Kang and G. Kotliar, *Phys. Rev. Materials* **2**, 034604 (2018).
- ²⁵⁸Y. Liu, C.-J. Kang, E. Stavitski, Q. Du, K. Attenkofer, G. Kotliar, and C. Petrovic, *Phys. Rev. B* **97**, 155202 (2018).
- ²⁵⁹X. He, D. J. Singh, P. Boon-on, M.-W. Lee, and L. Zhang, *J. Am. Chem. Soc.* **140**, 18058 (2018).
- ²⁶⁰Y. Fu and D. J. Singh, *Phys. Rev. Materials* **2**, 094408 (2018).
- ²⁶¹H. Zhu, R. He, J. Mao, Q. Zhu, C. Li, J. Sun, W. Ren, Y. Wang, Z. Lui, Z. Tang, A. Sotnikov, Z. Wang, D. Broido, D. J. Singh, G. Chen, K. Nielsch, and Z. Ren, *Nat. Commun.* **9**, 2497 (2018).
- ²⁶²H. Zhu, J. Mao, Y. Li, J. Sun, Y. Wang, Q. Zhu, G. Li, Q. Song, J. Zhou, Y. Fu, R. He, T. Tong, Z. Liu, W. Ren, L. You, Z. Wang, J. Luo, A. Sotnikov, J. Bao, K. Nielsch, G. Chen, D. J. Singh, and Z. Ren, *Nat. Commun.* **10**, 270 (2019).
- ²⁶³R. Matsumoto, M. Nagao, M. Ochi, H. Tanaka, H. Hara, S. Adachi, K. Nakamura, R. Murakami, S. Yamamoto, T. Irifune, H. Takeya, I. Tanaka, K. Kuroki, and Y. Takano, *J. Appl. Phys.* **125**, 075102 (2019).
- ²⁶⁴K. Terashima, Y. Yano, E. Paris, Y. Goto, Y. Mizuguchi, Y. Kamihara, T. Wakita, Y. Muraoka, N. L. Saini, and T. Yokoya, *J. Appl. Phys.* **125**, 145105 (2019).
- ²⁶⁵W. Feng, D. Xiao, Y. Zhang, and Y. Yao, *Phys. Rev. B* **82**, 235121 (2010).
- ²⁶⁶W. Feng, D. Xiao, J. Ding, and Y. Yao, *Phys. Rev. Lett.* **106**, 016402 (2011).
- ²⁶⁷W. Feng, W. Zhu, H. H. Weitering, G. M. Stocks, Y. Yao, and D. Xiao, *Phys. Rev. B* **85**, 195114 (2012).
- ²⁶⁸Z. Zhu, Y. Cheng, and U. Schwingenschlögl, *Phys. Rev. B* **85**, 235401 (2012).
- ²⁶⁹L. A. Agapito, N. Kioussis, W. A. Goddard, III, and N. P. Ong, *Phys. Rev. Lett.* **110**, 176401 (2013).
- ²⁷⁰X.-L. Sheng, Z. Wang, R. Yu, H. Weng, Z. Fang, and X. Dai, *Phys. Rev. B* **90**, 245308 (2014).
- ²⁷¹S. Küfner and F. Bechstedt, *Phys. Rev. B* **91**, 035311 (2015).
- ²⁷²J. Li, C. He, L. Meng, H. Xiao, C. Tang, X. Wei, J. Kim, N. Kioussis, G. M. Stocks, and J. Zhong, *Sci. Rep.* **5**, 14115 (2015).
- ²⁷³F. Arnold, C. Shekhar, S.-C. Wu, Y. Sun, R. D. dos Reis, N. Kumar, M. Naumann, M. O. Ajeesh, M. Schmidt, A. G. Grushin, J. H. Bardarson, M. Baenitz, D. Sokolov, H. Borrmann, M. Nicklas, C. Felser, E. Hassinger, and B. Yan, *Nat. Commun.* **7**, 11615 (2016).
- ²⁷⁴C.-J. Kang, J. D. Denlinger, J. W. Allen, C.-H. Min, F. Reinert, B. Y. Kang, B. K. Cho, J.-S. Kang, J. H. Shim, and B. I. Min, *Phys. Rev. Lett.* **116**, 116401 (2016).
- ²⁷⁵P. M. R. Brydon, L. Wang, M. Weinert, and D. F. Agterberg, *Phys. Rev. Lett.* **116**, 177001 (2016).
- ²⁷⁶J. Ruan, S.-K. Jian, D. Zhang, H. Yao, H. Zhang, S.-C. Zhang, and D. Xing, *Phys. Rev. Lett.* **116**, 226801 (2016).
- ²⁷⁷W. Cao, P. Tang, Y. Xu, J. Wu, B.-L. Gu, and W. Duan, *Phys. Rev. B* **96**, 115203 (2017).
- ²⁷⁸L.-Y. Rong, J.-Z. Ma, S.-M. Nie, Z.-P. Lin, Z.-L. Li, B.-B. Fu, L.-Y. Kong, X.-Z. Zhang, Y.-B. Huang, H.-M. Weng, T. Qian, H. Ding, and R.-Z. Tai, *Sci. Rep.* **7**, 6133 (2017).
- ²⁷⁹F. Arnold, M. Naumann, S.-C. Wu, Y. Sun, M. Schmidt, H. Borrmann, C. Felser, B. Yan, and E. Hassinger, *Phys. Rev. Lett.* **117**, 146401 (2016).
- ²⁸⁰Y. Quan, Z. P. Yin, and W. E. Pickett, *Phys. Rev. Lett.* **118**, 176402 (2017).
- ²⁸¹H. Oinuma, S. Souma, D. Takane, T. Nakamura, K. Nakayama, T. Mitsuhashi, K. Horiba, H. Kumigashira, M. Yoshida, A. Ochiai, T. Takahashi, and T. Sato, *Phys. Rev. B* **96**, 041120(R) (2017).
- ²⁸²X. Zhang, L. Jin, X. Dai, and G. Liu, *J. Phys. Chem. Lett.* **8**, 4814 (2017).
- ²⁸³H. Kim, K. Wang, Y. Nakajima, R. Hu, S. Ziemak, P. Syers, L. Wang, H. Hodovanets, J. D. Denlinger, P. M. R. Brydon, D. F. Agterberg, M. A. Tanatar, R. Prozorov, and J. Paglione, *Sci. Adv.* **4**, eaao4513 (2018).
- ²⁸⁴A. Parveen, E. Narsimha Rao, B. Adivaiah, P. Anees, and G. Vaitheeswaran, *Phys. Chem. Chem. Phys.* **20**, 5084 (2018).
- ²⁸⁵F. Tang, H. C. Po, A. Vishwanath, and X. Wan, *Nature* **566**, 486 (2019).
- ²⁸⁶Y. Li and D. J. Singh, *Phys. Rev. Materials* **1**, 075402 (2017).
- ²⁸⁷S. Zhang, H. Y. Xiao, S. M. Peng, G. X. Yang, Z. J. Liu, X. T. Zu, S. Li, D. J. Singh, L. W. Martin, and L. Qiao, *Phys. Rev. Applied* **10**, 044004 (2018).
- ²⁸⁸Y. Li and D. J. Singh, *J. Mater. Chem. C* **7**, 2436 (2019).
- ²⁸⁹K. Choudhary, Q. Zhang, A. C. Reid, S. Chowdhury, N. Van Nguyen, Z. Z. Trautt, M. W. Newrock, F. Y. Congo, and F. Tavazza, *Sci. Data* **5**, 180082 (2018).
- ²⁹⁰K. Choudhary, M. Bercx, J. Jiang, R. Pachter, D. Lamoén, and F. Tavazza, *Chem. Mater.* **31**, 5900 (2019).
- ²⁹¹P. Miró, M. Audiffred, and T. Heine, *Chem. Soc. Rev.* **43**, 6537 (2014).
- ²⁹²F. A. Rasmussen and K. S. Thygesen, *J. Phys. Chem. C* **119**, 13169 (2015).
- ²⁹³H. Park, R. Mall, F. H. Alharbi, S. Sanvito, N. Tabet, H. Bensmail, and F. El-Mellouhi, *Phys. Chem. Chem. Phys.* **21**, 1078 (2019).
- ²⁹⁴W. Hetaba, P. Blaha, F. Tran, and P. Schattschneider, *Phys. Rev. B* **85**, 205108 (2012).
- ²⁹⁵X. Xu and H. Jiang, *J. Chem. Phys.* **150**, 034102 (2019).
- ²⁹⁶S. J. Clark and J. Robertson, *Phys. Rev. B* **82**, 085208 (2010).
- ²⁹⁷P. Borlido, M. A. L. Marques, and S. Botti, *J. Chem. Theory Comput.* **14**, 939 (2018).
- ²⁹⁸A. V. Terentjev, L. A. Constantin, and J. M. Pitarke, *Phys. Rev. B* **98**, 085123 (2018).
- ²⁹⁹Y.-C. Wang and H. Jiang, *J. Chem. Phys.* **150**, 154116 (2019).
- ³⁰⁰T. F. T. Cerqueira, M. J. T. Oliveira, and M. A. L. Marques, *J. Chem. Theory Comput.* **10**, 5625 (2014).
- ³⁰¹A. Lindmaa and R. Armiento, *Phys. Rev. B* **94**, 155143 (2016).